



Contents lists available at ScienceDirect

## Brain, Behavior, and Immunity

journal homepage: [www.elsevier.com/locate/ybrbi](http://www.elsevier.com/locate/ybrbi)

Full-length Article

## Scavenger Receptor-A deficiency impairs immune response of microglia and astrocytes potentiating Alzheimer's disease pathophysiology

Francisca Cornejo<sup>a</sup>, Marianne Vruwink<sup>a</sup>, Claudia Metz<sup>b,c</sup>, Paola Muñoz<sup>a</sup>, Nicole Salgado<sup>a</sup>, Joaquín Poblete<sup>a</sup>, María Estela Andrés<sup>d</sup>, Jaime Eugenin<sup>e</sup>, Rommy von Bernhardt<sup>a,\*</sup><sup>a</sup> Laboratorio de Neurociencia, Departamento de Neurología, Facultad de Medicina, Pontificia Universidad Católica de Chile, Santiago, Chile<sup>b</sup> Centro de Envejecimiento y Regeneración CARE, Pontificia Universidad Católica de Chile, Santiago, Chile<sup>c</sup> Facultad de Ciencia, Universidad San Sebastián, Santiago, Chile<sup>d</sup> Departamento de Biología Celular y Molecular, Facultad de Ciencias Biológicas, Pontificia Universidad Católica de Chile, Santiago, Chile<sup>e</sup> Facultad de Química y Biología, Departamento de Biología, Universidad de Santiago de Chile, USACH, Santiago, Chile

## ARTICLE INFO

## Article history:

Received 9 August 2017

Received in revised form 4 December 2017

Accepted 11 December 2017

Available online xxx

## Keywords:

Aging

Beta-amyloid plaques

Glial cells

Neurodegenerative diseases

Neuroinflammation

Scavenger receptor

## ABSTRACT

Late onset Alzheimer disease's (LOAD) main risk factor is aging. Although it is not well known which age-related factors are involved in its development, evidence points out to the involvement of an impaired amyloid- $\beta$  ( $A\beta$ ) clearance in the aged brain among possible causes. Glial cells are the main scavengers of the brain, where Scavenger Receptor class A (SR-A) emerges as a relevant player in AD because of its participation in  $A\beta$  uptake and in the modulation of glial cell inflammatory response. Here, we show that SR-A expression is reduced in the hippocampus of aged animals and APP/PS1 mice. Given that  $A\beta$  deposition increases in the aging brain, we generated a triple transgenic mouse, which accumulates  $A\beta$  and is knockout for SR-A (APP/PS1/SR-A<sup>-/-</sup>) to evaluate  $A\beta$  accumulation and the inflammatory outcome of SR-A depletion in the aged brain. The lifespan of APP/PS1/SR-A<sup>-/-</sup> mice was greatly reduced, accompanied by a 3-fold increase in plasmatic pro-inflammatory cytokines, and reduced performance in a working memory behavioral assessment. Microglia and astrocytes lacking SR-A displayed impaired oxidative response and nitric oxide production, produced up to 7-fold more pro-inflammatory cytokines and showed a 12-fold reduction in anti-inflammatory cytokines release, with conspicuous changes in lipopolysaccharide-induced glial activation. Isolated microglia from young and adult mice lacking SR-A showed a 50% reduction in phagocytic activity. Our results indicate that reduced expression of SR-A can deregulate glial inflammatory response and potentiate  $A\beta$  accumulation, two mechanisms that could contribute to AD progression.

© 2017 Elsevier Inc. All rights reserved.

## 1. Introduction

The aging of the population is a major challenge in public health due to the increasing prevalence of age-related chronic diseases, including several neurodegenerative diseases. Aging is characterized by a chronic inflammatory state (Franceschi et al., 2007) and is the most prevalent risk factor for developing Alzheimer's disease (AD). In addition, increasing evidence shows that impaired amyloid- $\beta$  ( $A\beta$ ) clearance and neuroinflammation are contributing factors for developing late onset Alzheimer's disease (LOAD)

(Gallina et al., 2015; Mawuenyega et al., 2010; McIntee et al., 2016; Patterson et al., 2015).

Glial cells are responsible for the innate immune response in the brain, being also involved in  $A\beta$  clearance, and have attracted attention in the last decade as mediators of the neuroinflammation observed in AD (Krabbe et al., 2013; Medeiros and LaFerla, 2013; Olabarria et al., 2010; Streit et al., 2009). There is robust evidence showing that microglia and astrocytes develop an inflammatory phenotype as the brain ages (Lucin and Wyss-Coray, 2009; Mosher and Wyss-Coray, 2014; Rozovsky et al., 1998), showing an impaired capability to respond correctly to different stimuli such as pathogen associated molecules, like lipopolysaccharide (LPS), and also  $A\beta$  (Frank et al., 2010; Lue et al., 2001; Tichauer et al., 2014). These observations led the proposal of new hypotheses placing glial dysregulation as a possible cause for AD (Rodríguez et al., 2016; von Bernhardt, 2007; von Bernhardt et al., 2015).

\* Corresponding author.

E-mail addresses: [fcornej@uc.cl](mailto:fcornej@uc.cl) (F. Cornejo), [claudia.metz@uss.cl](mailto:claudia.metz@uss.cl) (C. Metz), [pcmunoz@med.puc.cl](mailto:pcmunoz@med.puc.cl) (P. Muñoz), [nasalgad@uc.cl](mailto:nasalgad@uc.cl) (N. Salgado), [mandres@bio.puc.cl](mailto:mandres@bio.puc.cl) (M.E. Andrés), [jaime.eugenin@usach.cl](mailto:jaime.eugenin@usach.cl) (J. Eugenin), [rvonb@med.puc.cl](mailto:rvonb@med.puc.cl) (R. von Bernhardt).

<https://doi.org/10.1016/j.bbi.2017.12.007>

0889-1591/© 2017 Elsevier Inc. All rights reserved.

Scavenger receptors have emerged as important actors in AD pathophysiology (Cornejo and von Bernhardi, 2013; El Khoury et al., 1998); in especial Scavenger Receptor class A (SR-A), given their participation in A $\beta$  phagocytosis (Frenkel et al., 2013) and in the outcome of inflammatory activation of glial cells (Godoy et al., 2012; Murgas et al., 2014). Several studies have shown that SR-A deficiency induces accumulation of A $\beta$  (Frenkel et al., 2013; Lifshitz et al., 2013; Yang et al., 2011). Furthermore, there is evidence that neuroinflammation induced by increased A $\beta$  reduces SR-A expression in microglia (Hickman et al., 2008), which could result in a vicious cycle in which A $\beta$  uptake and regulation of glial response by SR-A become impaired, further inducing A $\beta$  accumulation and a pro-inflammatory environment in the brain. Even though the role of SR-A in A $\beta$  uptake is well established, little is known about the way SR-A orchestrates the glial response in the presence of A $\beta$ .

In agreement with previous reports, we observed a reduction in SR-A expression in the hippocampus of aged WT mice, reduction that in APP/PS1 mice was already present at young ages, suggesting that SR-A participation could be reduced by aging and A $\beta$  accumulation. Thus, we generated a triple transgenic mouse that accumulates A $\beta$  and is knockout for SR-A (APP/PS1/SR-A<sup>-/-</sup>), to elucidate the relevance of SR-A for A $\beta$  accumulation and glial inflammatory outcome in the aged brain. Here we show that SR-A deficiency resulted in impairments in the inflammatory response of microglia and astrocytes in a model of A $\beta$  accumulation both *in vivo* and *in vitro*. The absence of SR-A changed the production of reactive oxygen species (ROS) and nitric oxide (NO), the levels of pro- and anti-inflammatory cytokines, and the phagocytic activity of microglial cells. SR-A-deficient APP/PS1 mice showed a high mortality rate, high levels of plasmatic inflammatory cytokines at young ages, increased A $\beta$  plaques and CD68 expression in the hippocampus. Working memory was mildly impaired in APP/PS1/SR-A<sup>-/-</sup> mice assessed with the 6 arms radial water maze (6ARWM) behavioral test.

Given the fact that A $\beta$  is upregulated in aged primate brains (Zhao et al., 2016), and that A $\beta$  accumulation could reduce SR-A expression (Hickman et al., 2008), our results suggest that SR-A reduced expression together with A $\beta$  accumulation impair the immune response mediated by microglia and astrocytes, promoting a pro-inflammatory environment and a reduced A $\beta$  clearance, favoring a vicious cycle for AD development.

## 2. Materials and methods

### 2.1. Reagents

LPS (from *Escherichia coli* 0111:B4), Thioflavin S and antibody against  $\alpha$ -tubulin were purchased from Sigma (ThermoFisher, USA). HiLyte Fluor 555-labeled-A $\beta$ <sub>(1-42)</sub> was purchased from Anaspec (USA). Percoll was obtained from GE Healthcare Life Sciences (USA). The antibody against ionized calcium-binding adapter molecule 1 (Iba1) was from Wako (Japan). Antibody against glial fibrillary acidic protein (GFAP) and the fluorescent mounting medium were purchased from Dako (Agilent Technologies, Denmark). Antibody against SR-A was from R&D Systems (USA). Antibody against CD68 was from AbD Serotec (USA). Alexa Fluor 488-conjugated secondary antibody anti-rabbit, 5-(6)-chloromethyl-2',7'-dichlorodihydrofluorescein diacetate (CM-H<sub>2</sub>DCF DA) and Hoechst 33258 were from Molecular Probes (ThermoFisher, USA). ELISA kits for cytokine detection were purchased from eBioscience (Affymetrix, USA). Cell culture media, antibiotics and serum were purchased from Gibco (ThermoFisher, USA). Flow cytometry buffers Cytofix/Cytoperm and Perm/Wash were obtained from BD biosciences (USA).

### 2.2. Mice

APP/PS1 bi-transgenic mice (B6.Cg-Tg(APP<sup>swe</sup>,PSEN1<sup>dE9</sup>)85D bo/J, C57Bl6/J background) were purchased from Jackson Laboratories (USA). SR-A<sup>-/-</sup> and SR-A<sup>+/+</sup> mice (129/ICR background) were kindly facilitated by Dr. Guillermo Merino, and their developer, Dr. Tatsuhiko Kodama (Research Center for Advanced Science and Technology, University of Tokyo, Japan) and kept at the institutional animal facility. Mice were housed at a maximum density of 5 adult mice per cage, in a temperature-regulated room with a 12 h light/dark cycle, and with free access to food and water. APP/PS1/SR-A<sup>-/-</sup> triple transgenic mice were generated by backcrossing heterozygous APP/PS1 and homozygous SR-A<sup>-/-</sup> animals for more than 12 generations. Animals were genotyped after weaning (primers and genotyping examples in Supplemental Fig. S1a). All procedures were performed following the animal handling and bioethical requirements defined by the Pontificia Universidad Católica de Chile School of Medicine Ethics Committee and the National Institutes of Health guide for the care and use of Laboratory animals (NIH Publications No. 8023, revised 1978).

### 2.3. Glial cultures

Mixed glial cell cultures, containing astrocytes and microglia, were obtained from the cerebral cortex of 1-to-2 day old WT, APP/PS1, SR-A<sup>-/-</sup> or APP/PS1/SR-A<sup>-/-</sup> mice, as previously described (Giulian and Baker, 1986). Briefly, cortices were rinsed with Ca<sup>2+</sup>/Mg<sup>2+</sup>-free Hank's balanced salt solution (HBSS); meninges were removed, and tissue was minced and incubated with 0.25% trypsin-EDTA in HBSS at 37 °C for 10 min. The tissue was mechanically dissociated, and cells were seeded in 75 cm<sup>2</sup> cell culture flasks (one brain per flask) in Dulbecco's Modified Eagle's Medium DMEM/F12 supplemented with 10% fetal bovine serum (FBS), 100 U/ml penicillin and 100  $\mu$ g/ml streptomycin. Cultures were incubated in a water saturated, 5% CO<sub>2</sub> atmosphere at 37 °C.

After 14 days in culture, microglia were purified by differential adhesion with 60 mM Lidocaine at 37 °C for 10 min (Bronstein et al., 2013). Microglia were resuspended and seeded in a 1:1 mixture of supplemented DMEM/F12 and conditioned media (Conditioned culture medium was obtained from mixed glial cell cultures, centrifuged at 200 g for 10 min, and kept sterile for later use). After 24 h of seeding, the medium was replaced by fresh supplemented DMEM/F12. Astrocytes were purified by differential adhesion after trypsinization of the attached cells after the isolation of microglial cells. This procedure yield cultures that were highly enriched in astrocytes (95% or more) or microglia (over 99%). Cell identity was evaluated by immunocytochemistry against Iba1 (1:500) for microglia, and GFAP (1:500) to identify astrocytes (data not shown).

Glia were plated in 6-well plates at a density of  $2.5 \times 10^5$  cells per well for Western blot, in 96-well black plates with optical bottom at a density of  $4 \times 10^4$  cells per well for ROS detection, and in 24-well plates at a density of  $1 \times 10^5$  cells for NO and ELISA determination of cytokines. For immunofluorescence,  $4 \times 10^4$  cells were seeded on 12 mm glass coverslips.

### 2.4. Western blot

Hippocampal tissue was homogenized in ice-cold RIPA buffer (50 mM Tris-HCl, 150 mM NaCl, 1% Triton X-100, 0.1% SDS, and protease inhibitors, pH 7.5). Samples were separated by electrophoresis in 12% poly-acrylamide gels and transferred to a nitrocellulose membrane. After transference, the membrane was treated with blocking buffer (0.05% Tween 20, 5% milk in PBS) and then incubated with goat anti SR-A (1:500), and mouse anti  $\alpha$ -tubulin (1:1000) primary antibodies. Supplemental Fig. S1b

and S1c show the characteristic pattern of labeling for SR-A. The primary antibody was rinsed, and the membranes were incubated with the corresponding horseradish peroxidase-conjugated secondary antibody (1:2000). Densitometry was made with the Image studio software (LI-COR).

### 2.5. ELISA determination of cytokines

Production of cytokines was determined by ELISA, according to the manufacturer's protocol (eBioscience/Affymetrix). Plasma samples were obtained from 3- and 12-month-old mice. Approximately 800  $\mu$ l of total blood was obtained by transcardiac puncture. Plasma was separated by centrifugation at room temperature (RT, 1100 g for 20 min) and stored at  $-20^{\circ}\text{C}$  until analysis.

For the assessment of cytokines in brain parenchyma, mice were perfused with ice cold HBSS by transcardiac puncture. The brain was extracted, and the hippocampus was collected in ice-cold lysis buffer (50 mM Tris, 150 mM NaCl, 1 mM EDTA, and protease inhibitors, pH 7.4), sonicated and centrifuged at  $4^{\circ}\text{C}$  (14,000 g for 30 min). The supernatant was collected and stored at  $-20^{\circ}\text{C}$  until the ELISA was performed.

For the determination of cytokine production by glial cells in culture, microglia were stimulated for 24 h and astrocytes for 48 h with 1  $\mu\text{g}/\text{mL}$  LPS. Cell culture supernatants were collected and kept frozen until the assay.

For the assay, 100  $\mu$ l of sample was added to the ELISA plate coated with the capture antibody and incubated at  $4^{\circ}\text{C}$  overnight (ON). A standard curve was simultaneously made with recombinant cytokine. Detection antibodies were incubated at RT for 1 h, and the reaction was developed with avidin–HRP and substrate solution. Absorbency was measured at 450 nm with reference to 570 nm with the microplate reader Synergy HT (Biotek Instruments).

### 2.6. Behavioral tests

Behavioral performance was evaluated in 9-month-old mice with the Morris Water Maze (Vorhees and Williams, 2006). Before beginning behavioral assessment, the mice performed a training protocol, which lasted 4 days, with 5 trials per day. The first behavioral test performed after the training was Task Q. This test lasted 5 days, with 10 trials with a maximum duration of 60 s per trial. Each trial began by positioning the mouse in a different quadrant of the pool, and the time for the animal to reach the platform, which was always located in the same quadrant, was recorded (Savonenko et al., 2005). The latency time to reach the platform was recorded using the MENU2100 software (HVS image).

At last, the 6-arm radial water maze (6ARWM) was performed. This test lasted 4 days, with 8 trials of 120 s as the maximum time allowed per trial. The mouse was put on a different arm of the maze in each trial, but each day the platform was placed on a different arm.

### 2.7. Assessment of A $\beta$ plaques by immunohistochemistry and Thioflavin S staining

The mice were transcardially perfused with cold HBSS followed by 4% p-formaldehyde (PFA). The brains were maintained in PFA ON., and the next day they were placed in a 10% sucrose solution, and transferred to a 30% sucrose solution after 48 h. The brains were cut with a cryostat (Microm), obtaining 40  $\mu$ m thick coronal sections for immunolabelling. Briefly, sections were incubated in a solution of 3%  $\text{H}_2\text{O}_2$  + 10% Methanol for 1.5 h, and then blocked with 5% goat serum (GS) at RT for 1 h. Subsequently, the sections were incubated with anti-Iba1 (1:1000) or anti-CD68 (1:1000) antibodies at  $4^{\circ}\text{C}$  ON. The next day, sections were incubated with biotinylated secondary antibody (1:200) at RT for 2 h, and then

incubated with ABC solution (1:100) for 1 h, and later revealed with the DAB kit (Vector Laboratories). After completion of labeling, the slides were mounted, allowed to dry at RT for 48 h, rehydrated, and immersed in hematoxylin solution for 5 min. Finally, the slides were incubated with 1% Thioflavin S in 70% ethanol for 10 min, rinsed in 70% ethanol for 5 min and sealed with Dako fluorescent mount medium.

### 2.8. Stereological analysis

To quantify CD68-positive cells in the hippocampus, the coronal sections labeled by immunohistochemistry were analyzed by stereology (Golub et al., 2015). Briefly, the fractional area for CD68 was measured using a light microscope coupled to an interface having the Stereo Investigator software (MBF Biosciences), and each sample was measured through a thickness in the range of 20–24  $\mu$ m (Hou et al., 2012). The hippocampus boundary was drawn, and a  $600 \times 600$   $\mu$ m sampling site was selected. At each sampling site, a 10  $\mu$ m spacing counting frame was superimposed, and those markers that co-located with cells positive for CD68 labeling were considered as positive, while the remaining markers were labeled negative. The fraction of area of immunoreactivity was calculated as the number of positive markers divided by the total number of markers.

### 2.9. In vitro A $\beta$ uptake assay

To determine the ability of glial cells to uptake A $\beta$ , purified microglia were incubated with 1  $\mu\text{g}/\text{ml}$  non-fibrillar HiLyte Fluor 555-labeled-A $\beta_{(1-42)}$  in supplemented DMEM/F12 at  $37^{\circ}\text{C}$  for 3 h. Cells were washed with PBS containing 1 mM  $\text{CaCl}_2$ , and fixed with 2% PFA at RT for 30 min. Fixed cells were permeabilized with 0.2% Triton X-100 for 10 min, and labeled with a rabbit anti-Iba1 (1:500) antibody at  $4^{\circ}\text{C}$  ON, and later with Alexa Fluor 488-conjugated anti-rabbit (1:500) at RT for 3 h, to confirm microglia identity. As a final step, nuclei were stained with Hoechst for 10 min. The coverslips were washed and mounted with Dako fluorescent mount medium. Five fields were randomly photographed per coverslip (Olympus, Tokyo, Japan). The percentage of microglia positive for labeled A $\beta$  and the mean fluorescence by cell was assessed with the Image J software (NIH).

### 2.10. Flow cytometry

Microglia and astrocytes were obtained from the brain as previously described (von Bernhardt et al., 2011). Briefly, brain cortices from 3- and 12-month-old mice were homogenized and passed through 120 and 60  $\mu$ m mesh filters. Homogenates were disaggregated in digestion buffer (0.05% collagenase D, 100  $\mu\text{g}/\text{ml}$  TLCK and 5 U/ml DNase I in 10 ml HBSS) at  $37^{\circ}\text{C}$  for 30 min, and centrifuged at RT (170 g for 10 min). The pellet was resuspended in 3 ml of 37% Percoll and slowly laid in 3 ml 70% Percoll (Cardona et al., 2006). On the top of the tube, 3 ml of 30% Percoll was added, followed by 2 ml of HBSS. The gradient was centrifuged at RT (14,100 g for 20 min with no brake), and glial cells were carefully isolated from the 37%/70% interface.

#### 2.10.1. SRA expression

presence of SR-A in microglia and astrocytes was assessed by flow cytometry. Cells were centrifuged at  $4^{\circ}\text{C}$  (100 g for 5 min), incubated with BD Cytofix/Cytoperm buffer on ice for 20 min, and washed twice with BD Perm/Wash buffer. After blocking with 10% goat serum for 20 min, cells were incubated with rabbit anti-Iba1 or anti-GFAP (1:100) and with goat anti-SR-A (1:100) in ice for 30 min, washed twice with BD Perm/Wash buffer, and incubated with anti-rabbit Alexa Fluor 488 (1:100) and anti-goat Alexa Fluor 564 (1:100) for another 30 min. After two additional

washes, cells were resuspended in 500  $\mu$ l of PBS and counted in a BD FACSVerser flow cytometer (BD Biosciences).

### 2.10.2. Ex vivo phagocytic assay

cells were pre-treated with 1  $\mu$ g/ml LPS for 30 min with gentle agitation at 37  $^{\circ}$ C, and then incubated with 1  $\mu$ g/ml HiLyte Fluor 555-labeled-A $\beta$ <sub>(1-42)</sub>, in supplemented DMEM/F12 at 37  $^{\circ}$ C for 3 h. Cells were centrifuged at 4  $^{\circ}$ C (100 g for 5 min), incubated with BD Cytofix/Cytoperm buffer on ice for 20 min, and washed twice with BD Perm/Wash buffer. After blocking with 10% goat serum for 20 min, cells were incubated with rabbit anti-Iba1 or anti-GFAP (1:100) in ice for 30 min, washed twice with BD Perm/Wash buffer, and incubated with anti-rabbit Alexa Fluor 488 (1:100) for another 30 min. After two additional washes, cells were resuspended in 500  $\mu$ l of PBS and counted in a BD FACSVerser flow cytometer (BD Biosciences).

### 2.11. Determination of nitrite

Nitrite (NO<sub>2</sub><sup>-</sup>), a stable product of NO, was determined by the Griess assay (Pfeiffer et al., 1997). Briefly, microglia were stimu-

lated for 48 h and astrocytes for 72 h with 1  $\mu$ g/ml LPS. After stimulation, 50  $\mu$ l of the culture medium was mixed with 10  $\mu$ l of 0.25 M EDTA (pH 8.0) and 60  $\mu$ l of freshly prepared Griess reagent (20 mg N-[1-naphthyl]-ethylendiamine and 0.2 g sulphanimide dissolved in 20 ml of 5% w/v phosphoric acid) for the determination of NO<sub>2</sub><sup>-</sup> production. Calibration curves were established with 1–80  $\mu$ M NaNO<sub>2</sub>. The reaction between NO<sub>2</sub><sup>-</sup> and the Griess reagent yield a colored product, whose absorbency was measured at 570 nm in a microplate reader Synergy HT (Biotek Instruments).

### 2.12. Reactive oxygen species determination

Reactive Oxygen Species (ROS) production was assessed with the ROS-sensitive dye CM-H<sub>2</sub>DCF DA, which oxidation produces a fluorescent adduct that remains trapped within cells. Microglia and astrocytes were loaded with 10  $\mu$ M CM-H<sub>2</sub>DCF DA ON, and treated with 1  $\mu$ g/ml LPS at 37  $^{\circ}$ C for 1 h. CM-H<sub>2</sub>DCF DA was excited at 485 nm, and emitted fluorescence was measured at 530 nm in a microplate reader Synergy HT (Biotek Instruments) at 37  $^{\circ}$ C.

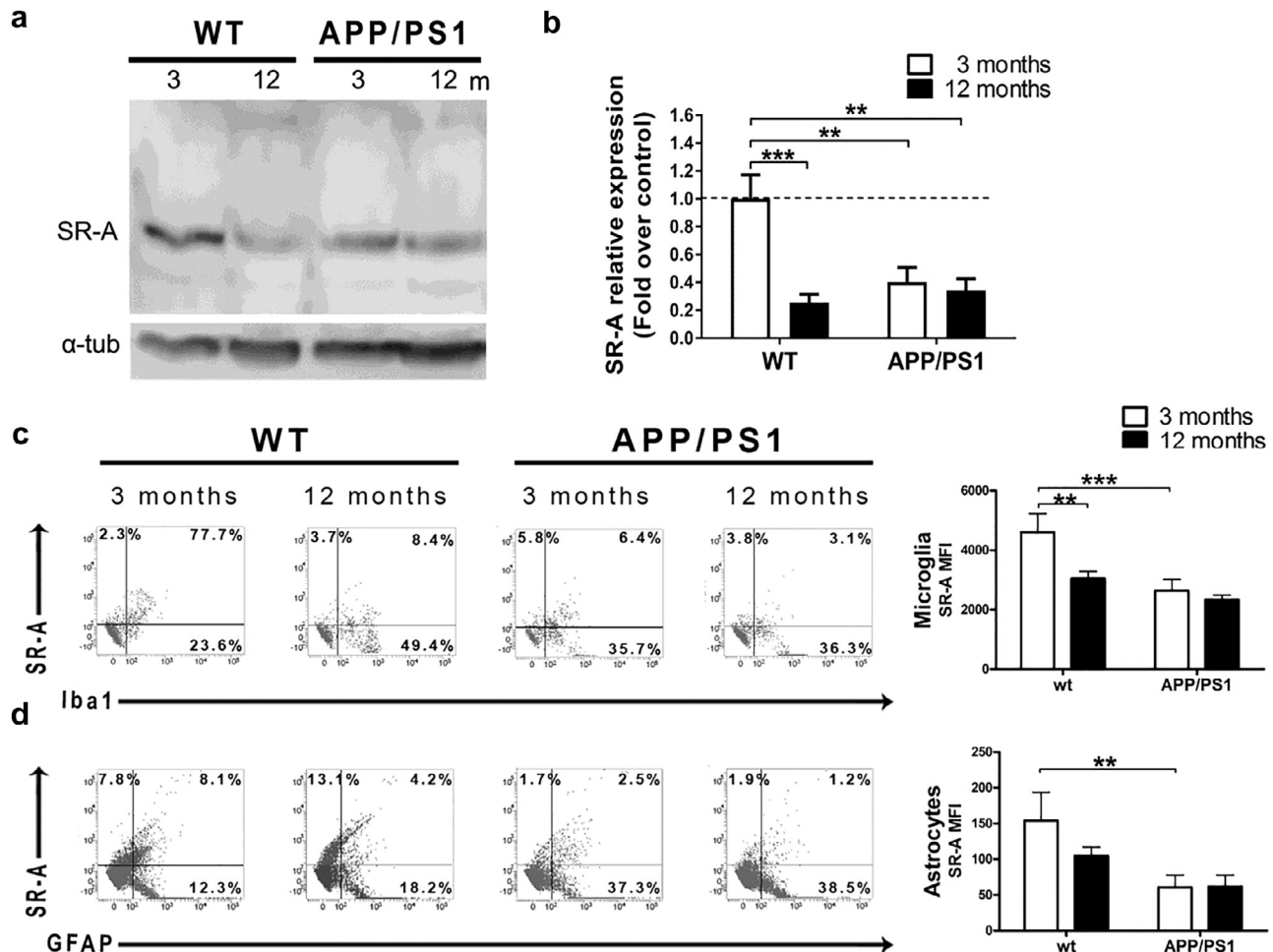


**Fig. 1.** SR-A expression is reduced in the hippocampus of APP/PS1 mice. (a) SR-A protein expression was measured in the hippocampus of 3- and 12-month-old WT and APP/PS1 mice by Western blot. (b) Results are expressed as the mean  $\pm$  SEM of the levels of SR-A normalized by  $\alpha$ -tubulin levels (as fold changes relative to the average value obtained from 3-month-old WT mice). Two-way ANOVA analysis revealed significant aging effect ( $F(1, 21) = 12.92, p = .0017$ ) and a significant effect of genotype ( $F(1,21) = 5.25, p = .0323$ ); \* and \*\*\* indicate  $p < .01$ , and  $p < .001$ , respectively using Bonferroni *post hoc* test. "n" at 3 months, WT = 7 (4F & 3 M); APP/PS1 = 6 (3F & 3 M); and at 12 months, WT = 6 (3F & 3 M); APP/PS1 = 7(4F & 4 M). Analysis of SR-A expression by flow cytometry showed that it is reduced in microglia (c) and astrocytes (d) of APP/PS1 and 12 months old WT mice. Results of microglial SR-A expression are shown as the relative intensity for SR-A labeling (MFI) on Iba1 positive cells  $\pm$  SEM (a). Results of hippocampal astrocytic SR-A expression are shown as relative intensity for SR-A labeling (MFI) on GFAP positive cells. Two-way ANOVA analysis for microglia revealed significant aging effect ( $F(1, 8) = 17.39, p = .0031$ ) and a significant effect for genotype ( $F(1,8) = 35.44, p = .0003$ ). For astrocytes, there was no significant effect for age ( $F(1,8) = 3.075, p = .1176$ ) but there was a significant effect for genotype ( $F(1,8) = 24.47, p = .0011$ ). \* and \*\*\* indicate  $p < .01$ , and  $p < .001$ , respectively using Bonferroni *post hoc* test. n = 3 per group.



### 2.13. Statistical analysis

Statistics were performed with two-way ANOVA analysis followed by Bonferroni's *post hoc* test to compare differences among genotypes (WT, APP/PS1, SR-A<sup>-/-</sup>, APP/PS1/SR-A<sup>-/-</sup>) at different experimental conditions (basal vs. LPS-treated mice, young vs. old mice). Non-parametric two-tailed statistics (Mann-Whitney test) was used to compare two independent samples. Sample sizes were defined based on previous studies and the requirements for specific two-tailed tests. All data were expressed as the mean ± SEM. Analyses were conducted with the GraphPad Prism software (GraphPad Software Inc). The null hypothesis was rejected if P < .05.

## 3. Results

### 3.1. Expression of SR-A is reduced in the hippocampus of APP/PS1 mice

To complement previous reports (Hickman et al., 2008), we measured SR-A expression in the hippocampus of WT and APP/PS1 mice by Western blot (Fig. 1a). We show that, whereas in 12-month-old WT mice, SR-A expression was reduced by 75% compared to 3-month-old WT, in APP/PS1 mice SR-A expression was already low in 3-month-old animals, being half of that of WT mice at 3 months of age. No changes were observed between 3- and 12-month-old APP/PS1 mice (Fig. 1b). To address changes in SR-A expression in microglia and astrocytes, glial cells were isolated from 3 and 12 months old WT and APP/PS1 mice, and SR-A expression was assessed by flow cytometry (Fig. 1c, d). A similar SR-A expression pattern profile to that observed in the hippocampus was observed in microglia across genotypes. Microglia and astrocytes from 3-month-old WT mice express higher SR-A amounts than 3- and 12-month-old APP/PS1 mice and 12 months old WT animals. The expression of SR-A by microglia is over 20-fold higher than in astrocytes (compare graphs in panels c and d). To establish if Aβ affects directly SR-A expression, we exposed neonatal glial cells in culture to increasing concentrations of Aβ (0.2 μm, 0.5 and 1 μm for 48 h). Our preliminary analysis with qPCR analysis showed a reduction on SR-A mRNA levels normalized with the RPLP0 ribosomal mRNA (Supplemental Fig. S2).

### 3.2. The absence of SR-A in APP/PS1 mice reduces life expectancy and increases the plasmatic level of inflammatory cytokines

To determine the effects of SR-A deficiency over the phenotypic features of APP/PS1 mice *in vivo*, physiological and inflammatory changes induced in APP/PS1/SR-A<sup>-/-</sup> mice were compared with WT or single transgenic mice. During the first two months of age, APP/PS1/SR-A<sup>-/-</sup> mice did not exhibit behavioral or phenotypic differences compared with the WT, APP/PS1 and SR-A<sup>-/-</sup> littermates. However, mortality increased abruptly around the third month and by the fifth month of life, approximately 60% APP/PS1/SR-A<sup>-/-</sup> mice were dead; whereas more than 95% mice of the other genotypes were still alive. By 12 months of age, only 10% of triple APP/PS1/SR-A<sup>-/-</sup> mice were alive (the maximal life span recorded was 13.9 months), whereas 90% or more mice of the other genotypes were alive. Although APP/PS1 and SR-A<sup>-/-</sup> mice showed a slight increase of mortality after 5 months of age, their life span showed no statistically significant difference with that of WT animals (Fig. 2a).

In addition, as an overall assessment of the health and welfare of mice, a veterinarian regularly performed a general body condition assessment and weight them at weaning and bi-weekly after 3 months of age. Our results show that there are no statistically significant differences in weight among the various genotypes

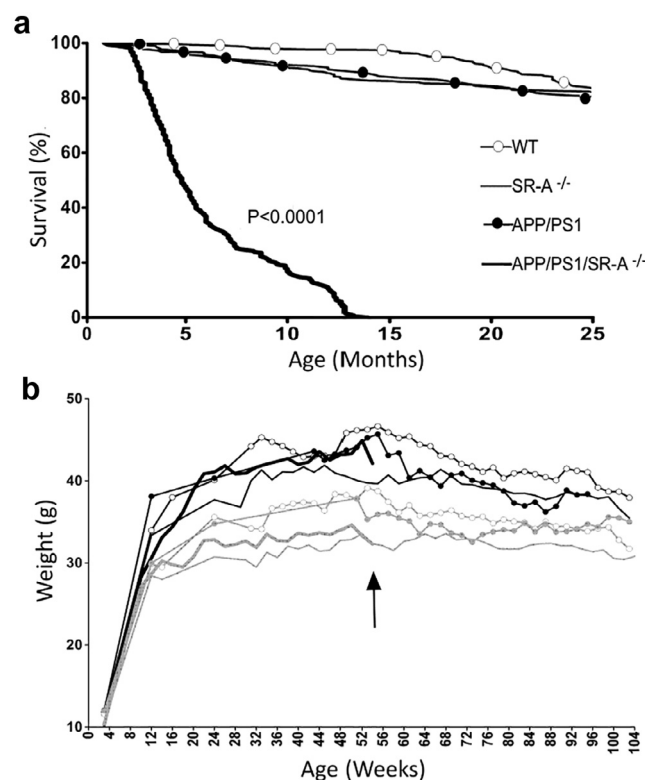


**Fig. 2.** APP/PS1/SR-A<sup>-/-</sup> mice have increased mortality. (a) Kaplan-Meier survival curves are shown for WT, APP/PS1, SR-A<sup>-/-</sup> and APP/PS1/SR-A<sup>-/-</sup> mice. P < .0001 for APP/PS1/SR-A<sup>-/-</sup> curve compared with the other genotypes according to Mantel-Cox test. The survival assessment started at 1 month of age. The number of mice used for the survival curves are as follow: WT n = 308, APP/PS1 n = 204, SR-A<sup>-/-</sup> n = 537, APP/PS1/SR-A<sup>-/-</sup> n = 252. Representation of females and males was similar, and no significant differences depending on sex were detected. (b) Development of body weight recorded bi-weekly in male (in black) and female (in grey) mice for the 4 genotypes. The arrow shows the period when the last APP/PS1/SR-A<sup>-/-</sup> mice die (thick black/grey line). There was no conspicuous weight loss in the triple transgenic animals. The number of mice evaluated for their weight is as follow: WT n = 27F & 24 M; APP/PS1 n = 13F & 12 M, SR-A<sup>-/-</sup> n = 25F & 27 M, APP/PS1/SR-A<sup>-/-</sup> n = 13F & 24 M.

(Fig. 2b; males in black and females in grey). Finally, table 1 shows the recorded cause of death. Although we observed a discrete increase of humane end in transgenic compared with WT animals, the most relevant cause of death for APP/PS1/SR-A<sup>-/-</sup> mice appeared to be sudden unexpected death during the night (a 23-fold increase compared with WT mice and 10-fold increase compared with SR-A<sup>-/-</sup> mice). The mice found dead did not show signs of deterioration. There was no rapid body weight loss, nor hypothermia, labored respiration, diarrhea, abnormal vocalization

**Table 1**  
Recorded cause of death during the 1st year of life.

	WT/ SRA <sup>+/+</sup> %	APP/PS1/ SRA <sup>+/+</sup> %	WT/ SRA <sup>-/-</sup> %	APP/PS1/ SRA <sup>-/-</sup> %
Humane end point				
Severe Dermatitis/Ocular Infections	0.0	2.3	2.0	2.2
Underdevelopment/ Deteriorating body condition	1.4	1.6	3.5	2.8
Prolapse (intestinal or genitourinary)	0.5	0.8	1.0	1.7
Total Humane end point	1.9	4.7	6.5	6.7
Found dead	3.4	9.4	7.6	79.2
Total	5.3	14.1	14.1	86.0

or posture, nor behaviors suggestive of acute stress that would activate the humane end point protocol. In terms of general behavior, APP/PS1/SR-A<sup>-/-</sup> mice showed repetitive behaviors, increased barbering, and very aggressive behavior especially among males older than 2 months old. We also received reports on behavior suggestive of seizures (coherent with the sudden unexpected death during the night) or other motor abnormalities, which we could not objectively evaluate, but were not reported for the other genotypes. Autopsy analysis on animals subjected to humane endpoint or some of those found dead did not reveal conspicuous changes explaining death (hemorrhage, conspicuous brain lesions or generalized infection processes).

To address pathophysiological alterations that could be related to the premature death of triple transgenic mice, we analyzed the plasmatic levels of inflammatory cytokines in young and adult mice (3- and 12-month-old, respectively, Fig. 3). Three months old APP/PS1/SR-A<sup>-/-</sup> mice had higher levels of IL1 $\beta$  and TNF $\alpha$  than APP/PS1 mice, which have similar levels than those in WT and SR-A<sup>-/-</sup>. At 12 months of age, SR-A<sup>-/-</sup> mice showed a significant increase of plasma levels of IL1 $\beta$  and TNF $\alpha$ , increase that was further exacerbated in the APP/PS1/SR-A<sup>-/-</sup> mice (Fig. 3). No significant differences were found between male and female mice (not shown).

### 3.3. Neurobehavioral performance in the 6ARWM test is impaired in APP/PS1/SR-A<sup>-/-</sup> mice

To analyze the effect of the absence of SR-A on the behavior of APP/PS1 mice, two neurobehavioral tests were performed:

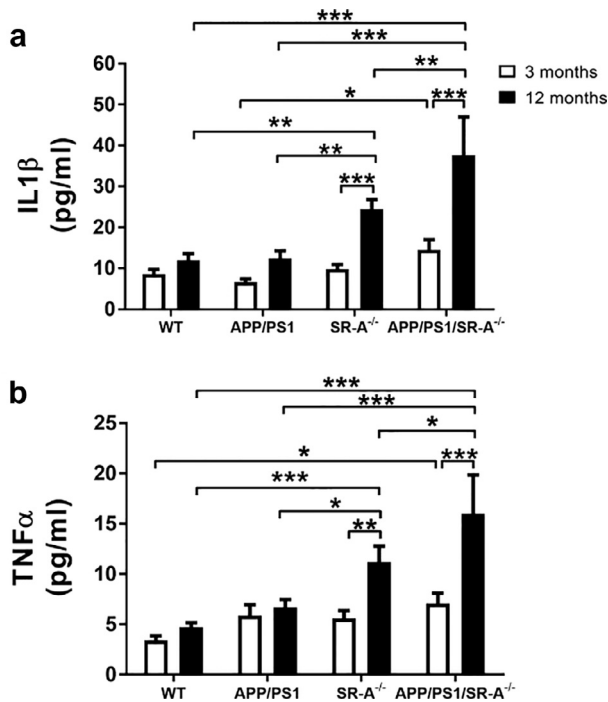


**Fig. 3.** The absence of SR-A results in increased plasmatic levels of inflammatory cytokines. IL1 $\beta$  (a) and TNF $\alpha$  (b) levels were measured in plasma obtained from blood drawn by transcardiac puncture from 3- and 12-month-old mice (white and black filled bars, respectively). Results are expressed as the mean  $\pm$  SEM of the cytokine concentration determined by ELISA. Two-way analysis revealed for IL1 $\beta$  plasmatic levels significant aging effect (df = 1,  $F$  ratio = 48.06,  $p < .0001$ ) and a significant effect of genotype (df = 3,  $F$  ratio = 19.3,  $p < .0001$ ). Likewise, two-way analysis revealed for TNF $\alpha$  plasmatic levels a significant effect of aging (df = 1,  $F$  ratio = 25.65,  $p < .0001$ ) and a significant effect of genotype (df = 3,  $F$  ratio = 13.83,  $p < .0001$ ); \*, \*\*, and \*\*\* indicate  $p < .05$ ,  $p < .01$ , and  $p < .001$ , respectively using Bonferroni *post hoc* test. "n" at 3 months, WT = 18 (9F & 9M), APP/PS1 = 22 (12F & 10M), SR-A<sup>-/-</sup> = 19 (9F & 10M), APP/PS1/SR-A<sup>-/-</sup> = 15 (8F & 7M) and at 12 months, WT = 20 (10F & 10M), APP/PS1 = 13 (6F & 7M), SR-A<sup>-/-</sup> = 15 (8F & 7M), APP/PS1/SR-A<sup>-/-</sup> = 9 (4F & 5M).

6ARWM, which evaluates working memory and Task Q, which evaluates spatial memory (Fig. 4). Analysis of the latency time in the Task Q showed significant differences for the APP/PS1 mice at the first day (Fig. 4a). Also, on the 6ARWM test, it took longer for APP/PS1/SR-A<sup>-/-</sup> mice to find the platform compared with WT mice on day 2 of the assay, when the animals presented the worst behavioral performance (Fig. 4b).

### 3.4. APP/PS1/SR-A<sup>-/-</sup> mice have an increased deposition of A $\beta$ plaques in the hippocampus

To evaluate the effect of the absence of SR-A on the formation of A $\beta$  plaques, hippocampal cryosections of APP/PS1 and APP/PS1/SR-A<sup>-/-</sup> mice were labeled with Thioflavin S to visualize the A $\beta$  plaques (Fig. 5a, b). Measurement of the area occupied by A $\beta$  plaques revealed that APP/PS1/SR-A<sup>-/-</sup> animals had twice as much area occupied by A $\beta$  plaques than that observed in the hippocampus of APP/PS1 mice, also having a significant increase in the number of A $\beta$  plaques (Fig. 5c). The area occupied by A $\beta$  plaques is similarly increased in APP/PS1 and APP/PS1/SR-A<sup>-/-</sup> mice at 9 months (Fig. 5a,b,e,f), but differences were observed in the number of A $\beta$  plaques with age (Fig. 5b,g). In contrast, no significant differences were found in the number of microglia associated with each A $\beta$

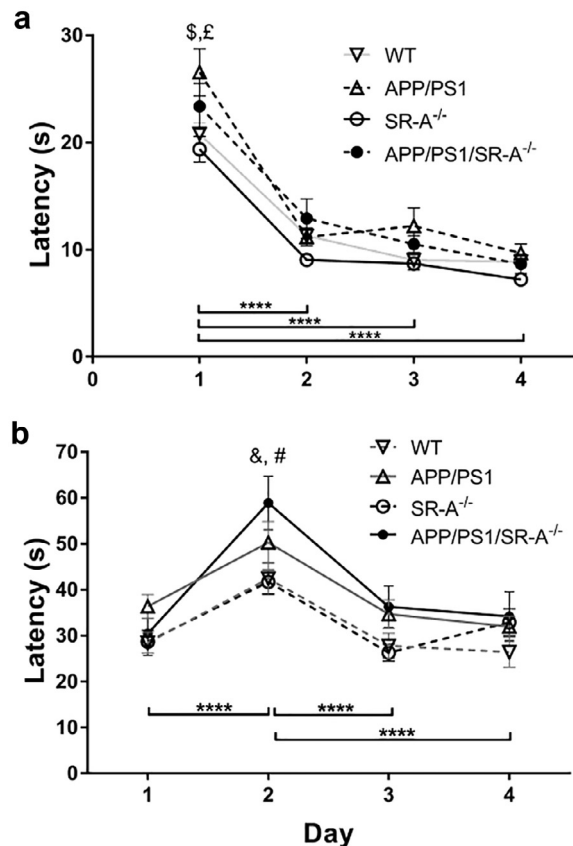


**Fig. 4.** APP/PS1/SR-A<sup>-/-</sup> mice have reduced working memory. Latency time was measured for the Task Q (a) and for the 6ARWM (b). In a, Two-way ANOVA analysis with repeated measurements revealed significant days of training effect ( $F(3, 231) = 148.6$ ,  $p < .0001$ ) and a significant effect of genotype ( $F(3, 77) = 5.921$ ,  $p < .0011$ ); "\$" indicates  $p = .0025$  between APP/PS1 and WT, and "E" indicates  $p < .0031$  between APP/PS1 and SR-A<sup>-/-</sup>. In b, ANOVA two-way analysis with repeated measurements revealed significant days of training effect ( $F(3, 231) = 29.12$ ,  $p < .0001$ ) and a significant effect of genotype ( $F(3, 77) = 4.661$ ,  $p < .0048$ ); \*\*\*\* indicates  $p < .0001$ ; "&" indicates  $p = .0103$  between APP/PS1/SR-A<sup>-/-</sup> and WT, and "#" indicates  $p = .0031$  between APP/PS1/SR-A<sup>-/-</sup> and SR-A<sup>-/-</sup>. Multiple comparisons were performed with Bonferroni *post hoc* test; WT = 20 (10F & 10M), APP/PS1 = 23 (11F & 12M), SR-A<sup>-/-</sup> = 27 (13F & 14M), APP/PS1/SR-A<sup>-/-</sup> = 15 (6F & 9M).

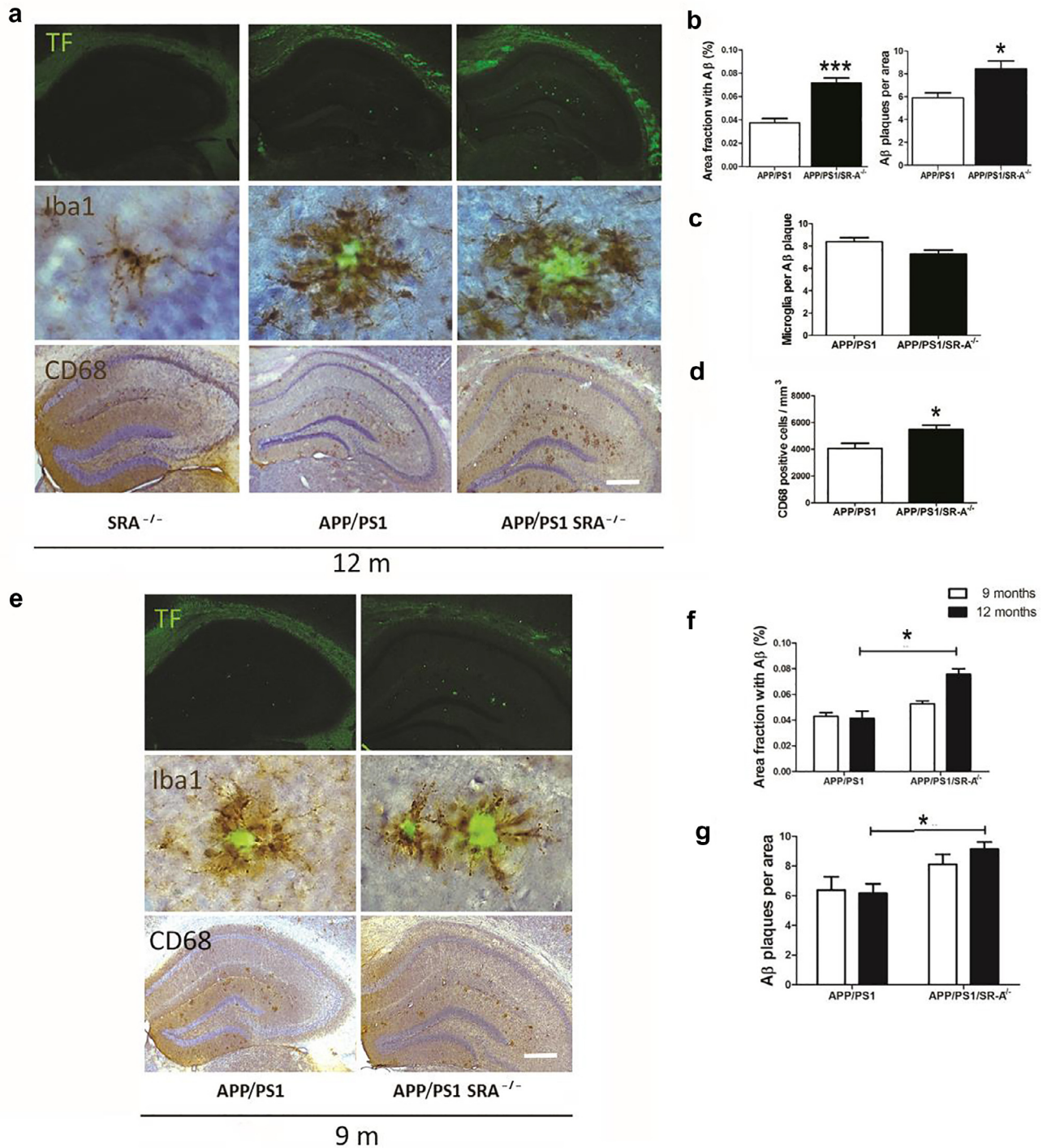


**Fig. 5.** APP/PS1/SR-A<sup>-/-</sup> mice have an increased deposition of A $\beta$  plaques in the hippocampus at 9 and 12 months. The area of A $\beta$  plaques in the hippocampus of APP/PS1 and APP/PS1/SR-A<sup>-/-</sup> mice were measured at (a) 12 months and (e) 9 months of age in thioflavin S (TF, green) stained sections (Scale bar = 200  $\mu$ m). The results are shown as the percentage of area occupied by A $\beta$  plaques per area of hippocampus and as number of A $\beta$  plaques per field (b, f, g). The number of microglia (brown) associated with each hippocampal A $\beta$  plaque (green) in APP/PS1 and APP/PS1/SR-A<sup>-/-</sup> mice were assessed by immunohistochemistry against Iba1 in 9 and 12-month-old mice (scale bar = 20  $\mu$ m). The results are shown as the number of microglia per A $\beta$  plaque (c). The number of phagocytic cells in the hippocampus of APP/PS1 and APP/PS1/SR-A<sup>-/-</sup> mice were determined at 9 and 12 months of age by immunohistochemistry against CD68 (brown) in hippocampal cryosections (scale bar = 200  $\mu$ m). The results of the stereological quantification are shown as the number of cells positive for CD68 per mm<sup>3</sup> (d). A comparative analysis of CD68 presence in the hippocampus at 12-month old mice of the different genotypes showed that SR-A<sup>-/-</sup> and WT microglia showed similar levels of CD68 expression. In contrast, CD68 in APP/PS1 hippocampus was 1.8-fold higher and in APP/PS1 SR-A<sup>-/-</sup> was 2.4-fold higher than in WT animals (Supplemental Fig. S3). Data correspond to the mean  $\pm$  SEM. Differences in area and number of plaques (b) and number of CD68 positive cells (d) are  $p < .05$  and  $***p < .001$  according to Mann-Whitney test. Two-way ANOVA analysis showed significant effect of the genotype ( $F(3,18) = 19.34$ ,  $p = .0083$ ), but not for age ( $F(1,18) = 0.1349$ ,  $p < .1934$ ). The difference in plaque area between APP/PS1 and APP/PS1/SR-A<sup>-/-</sup> has  $p < .05$  at 12 months of age. n: WT = 7 (4F & 3M), APP/PS1 = 8 (4F & 4M), SR-A<sup>-/-</sup> = 7 (3F & 4M), APP/PS1/SR-A<sup>-/-</sup> = 7 (4F & 3M).



plaque among phenotypes (Fig. 5c), although a significant increase in the number of microglia CD68 positive was observed at 12 months in the hippocampus of APP/PS1/SR-A<sup>-/-</sup> mice (Fig. 5a, d, Supplemental Fig. S3).

### 3.5. Microglia isolated from mice lacking SR-A show a reduced uptake of A $\beta$

Primary cultures of microglia were seeded in coverslips and incubated with fluorescently-tagged A $\beta_{(1-42)}$  (Cy3-A $\beta$ ) to determine their phagocytic capacity (Fig. 6). There was a strong influence of SR-A deficiency on morphology. SR-A-deficient microglia appeared in a rather small and elongated shape, even after stimulation with LPS, whereas WT and APP/PS1 microglia displayed

the typical shape of activated amoeboid microglia. Most of microglia derived from WT and APP/PS1 mice actively up-took A $\beta$  (Fig. 6a, b) in unstimulated conditions. By contrast, in unstimulated conditions cells lacking SR-A (SR-A<sup>-/-</sup> and APP/PS1/SR-A<sup>-/-</sup>) showed a 20% reduction of cells phagocytosing A $\beta$  (Fig. 6c, e). When microglia were previously treated with LPS, A $\beta$  phagocytosis (measured as the mean fluorescence per cell) was only induced in APP/PS1 cells, but induction was abolished in APP/PS1/SR-A<sup>-/-</sup> (Fig. 6j), suggesting that lack of SR-A impaired A $\beta$  uptake induction by LPS in APP/PS1 microglia. Cy3-A $\beta$  and Iba1 antibody shared the same plane localization in confocal analysis (Fig. 6k-n). The Z-scan images taken to verify A $\beta$  uptake revealed that the Cy3-A $\beta$  was internalized by microglial cells and not bound to the cell surface (Fig. 6k-n).

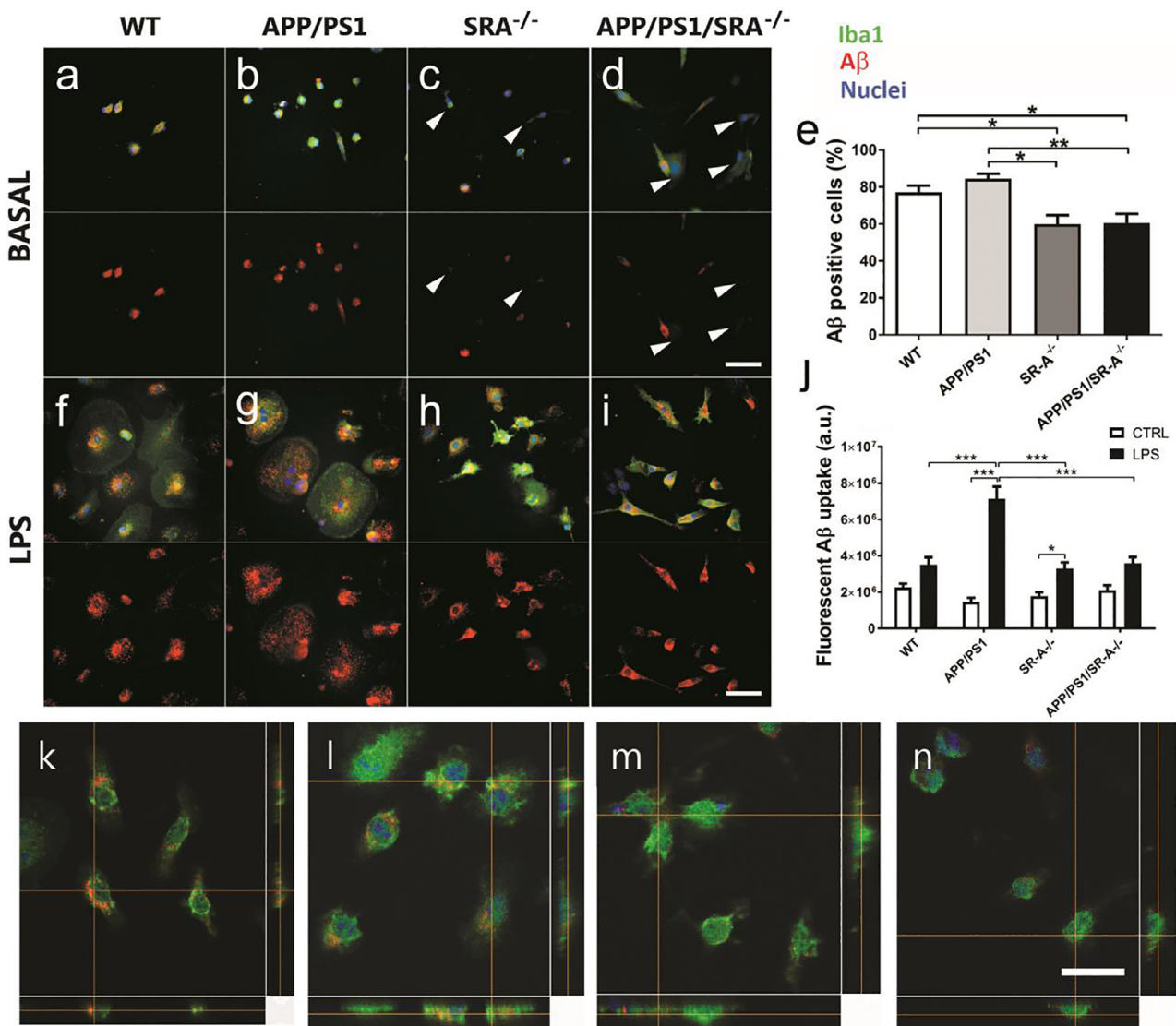


**Fig. 6.** A $\beta$  phagocytosis is reduced in the absence of SR-A. Purified microglia were incubated with fluorescently-tagged A $\beta_{(1-42)}$  (Cy3-A $\beta$ ) for 3 h (red label). The number of microglia that phagocytosed A $\beta$  in basal conditions (a-d) and after LPS treatment (e-i) varied according microglia was obtained from WT (a, f, k), APP/PS1 (b, g, l), SR-A<sup>-/-</sup> (c, h, m) and APP/PS1/SR-A<sup>-/-</sup> (d, i, n) mice. Microglia was identified by immunofluorescence against Iba1 (green label). Arrow heads show cells that are negative for A $\beta$ . The average of the percentage of A $\beta$  positive microglia cells (e) is reduced in mice lacking SR-A ( $p = .0070$ ,  $df = 3$  followed by Newman-Keuls *post hoc* test); Two way ANOVA analysis revealed a significant effects of LPS treatment for 48 h ( $df = 1$ ,  $F = 75.90$ ,  $p < .0001$ ) and genotype ( $df = 3$ ,  $F = 9.068$ ,  $p < .0001$ ) upon the A $\beta$ -fluorescence of microglia cells (j); values are expressed as the mean  $\pm$  SEM. (e) \*, \*\*, and \*\*\* indicate  $p < .05$ ,  $p < .01$ , and  $p < .001$  in Newman-Keuls and Bonferroni *post hoc* tests. (k-n) Confocal images of immunolabelled assays of Cy3-A $\beta$  phagocytosed by WT (k), APP/PS1 (l), SR-A<sup>-/-</sup> (m) and APP/PS1/SR-A<sup>-/-</sup> (n) microglia. Uptake of Cy3-A $\beta$  (Red) and immunofluorescence against Iba1 (green) were in the same z-plane compartment of the cell, suggesting Cy3-A $\beta$  incorporation into the cell. Nuclei are labeled with Hoechst (blue). Planes YZ and XZ are also shown. Orange lines indicate corresponding points on the orthogonal planes, showing localization of the label within the pictured cell. Scale bar = 20  $\mu$ m. Microglia cultures were obtained from pools of neonates obtained from independent mothers. n: WT = 5, APP/PS1 = 5, SR-A<sup>-/-</sup> = 6, APP/PS1/SR-A<sup>-/-</sup> = 3.



Cortical glial cells freshly isolated from young and adult mice were incubated with fluorescent-tagged A $\beta$  to test their ability to uptake A $\beta$  by flow cytometry (Fig. 7). Microglia obtained from 3-

month-old WT and APP/PS1 mice showed a higher capacity to phagocytose A $\beta$  than their SR-A $^{-/-}$  and APP/PS1/SR-A $^{-/-}$  counterparts (Fig. 7a, b). A 50% decrease in the ability to phagocytose A $\beta$

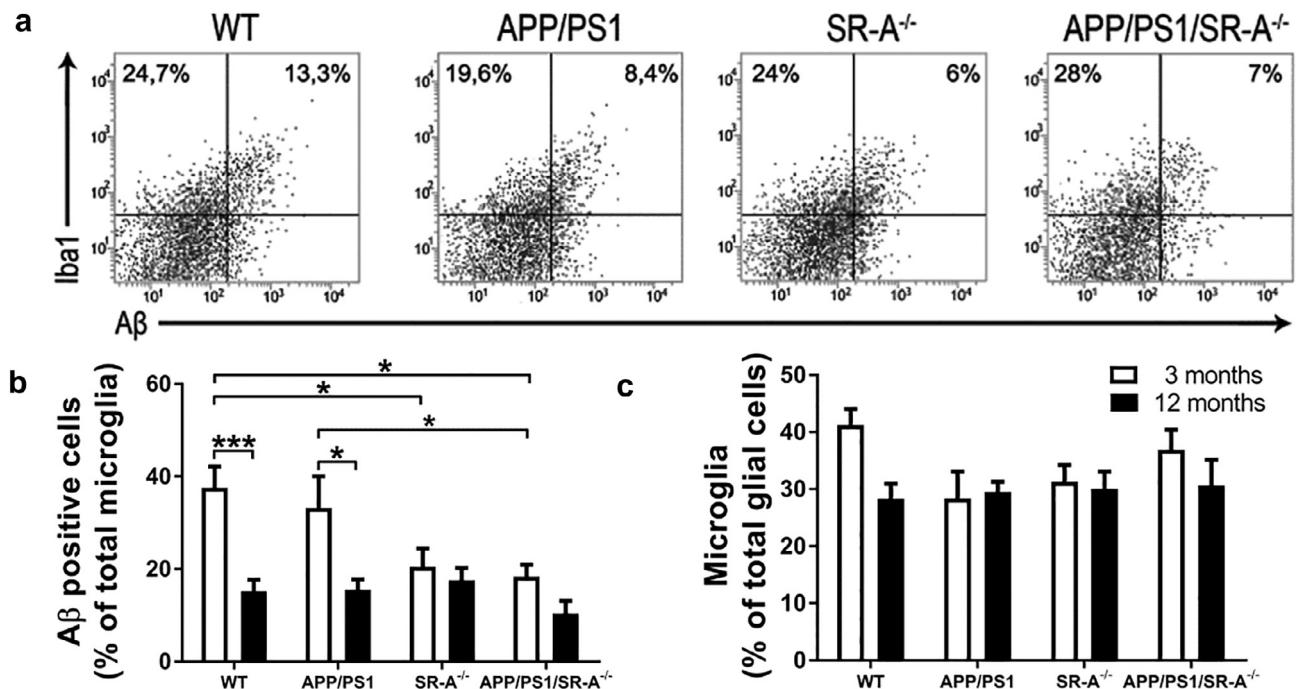


**Fig. 7.** A $\beta$  phagocytosis in microglia obtained from young mice is reduced in the absence of SR-A. Microglia and astrocytes were isolated from 3- and 12-month-old mice. The capacity of microglia to phagocytose A $\beta$  was assessed by flow cytometry with a phagocytosis assay using fluorescent-tagged A $\beta$ . (a) Representative dot plots obtained from 3-month-old mice are shown for each genotype. (b) Results of microglial phagocytosis are shown as the mean of Iba1 and A $\beta$  positive cells respective to the total number of Iba1 positive cells  $\pm$  SEM; Two-way ANOVA analysis revealed significant effect of age ( $F(1,92) = 24.27, p < .0001$ ) and genotype ( $F(3,92) = 4.15, p = .0083$ ). In c, the percentage of microglia respect to the total number of glial cells are shown. Two-way ANOVA revealed no significant effect for both, age ( $F(1, 76) = 3.755, p = .0564$ ) and genotype ( $F(3,76) = 1.185, p = .3211$ ). Values in b and c, are expressed as the mean  $\pm$  SEM. \*, \*\*, and \*\*\* indicate  $p < .05, p < .01, and p < .001$  in Bonferroni *post hoc* test. 3 months: WT  $n = 13$ , APP/PS1  $n = 17$ , SR-A $^{-/-}$   $n = 15$ , APP/PS1/SR-A $^{-/-}$   $n = 11$ . 12 months: WT  $n = 22$ , APP/PS1  $n = 19$ , SR-A $^{-/-}$   $n = 27$ , APP/PS1/SR-A $^{-/-}$   $n = 8$ .

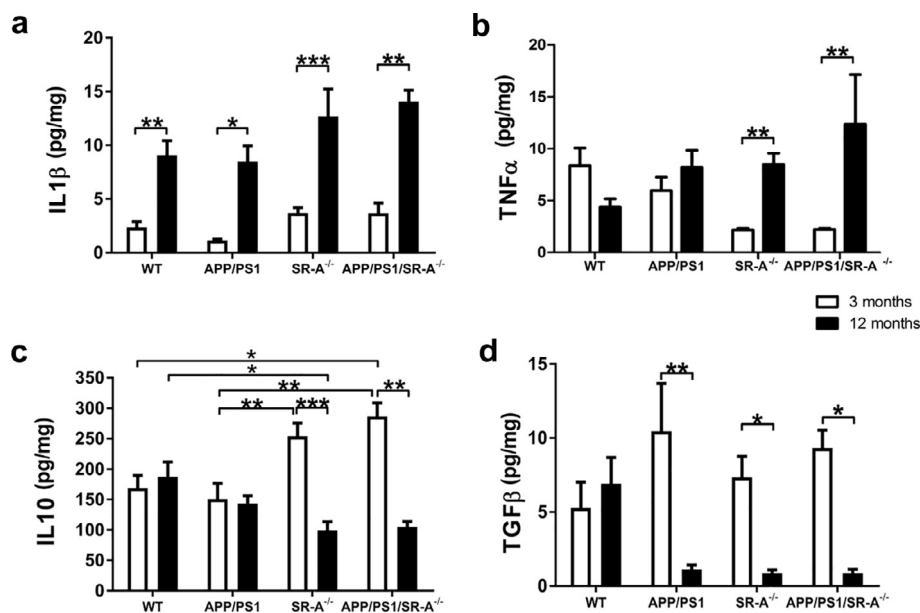


**Fig. 8.** The cytokine profile in the hippocampus is affected by the presence of SR-A. IL1 $\beta$  (a), TNF $\alpha$  (b), IL10 (c) and TGF $\beta$  (d) levels were measured *ex vivo* in the hippocampus of 3- and 12-month-old mice. Results are shown as the mean  $\pm$  SEM of the concentration expressed as picograms of cytokine per milligram of protein in the tissue. Two-way ANOVA analysis show significant effect of age for IL1 $\beta$  ( $F(1,48) = 75.66, p < .0001$ ), TNF $\alpha$  ( $F(1, 24) = 11.52, p < .0001$ ), IL10 ( $F(1, 79) = 23.48, p < .0001$ ), and TGF $\beta$  ( $F(1, 92) = 22.79, p < .0001$ ). Significant effect of genotype was observed for IL10 ( $F(3, 79) = 14.28, p = .0241$ ), but not for IL1 $\beta$  ( $F(3,48) = 0.7468, p = .5295$ ), TNF $\alpha$  ( $F(3, 124) = 0.73, p = .5352$ ), and TGF $\beta$  ( $F(3, 92) = 0.6072, p = .6120$ ); \*, \*\*, and \*\*\* indicate  $p < .05, p < .01, and p < .001$ , respectively, for multiple comparisons with Bonferroni *post hoc* test. 3 months: WT  $n = 13$ , APP/PS1  $n = 17$ , SR-A $^{-/-}$   $n = 15$ , APP/PS1/SR-A $^{-/-}$   $n = 11$ . 12 months: WT  $n = 22$ , APP/PS1  $n = 19$ , SR-A $^{-/-}$   $n = 27$ , APP/PS1/SR-A $^{-/-}$   $n = 8$ .

was observed in 12-month-old WT and APP/PS1 compared with the young mice (Fig. 7b), even though the fraction of microglia in the glial cell population was unaffected by the age or the genotype of the mice (Fig. 7c).

### 3.6. The absence of SR-A modifies IL1 $\beta$ , TNF $\alpha$ and IL10 levels in the hippocampus

Pro- and anti-inflammatory cytokine levels were assessed in the hippocampus of young and adult mice. Hippocampal levels of IL1 $\beta$  increased significantly in 12-month-old mice, where SR-A<sup>-/-</sup> showed higher levels compared with SR-A<sup>+/+</sup> mice (Fig. 8a). Interestingly, 3-month-old SR-A<sup>-/-</sup> and APP/PS1/SR-A<sup>-/-</sup> mice had low levels of TNF $\alpha$  in the hippocampi, which increased above the levels of WT animals at 12 months of age (Fig. 8b). Regarding anti-inflammatory cytokines, 3-month-old mice lacking SR-A (SR-A<sup>-/-</sup> and APP/PS1/SR-A<sup>-/-</sup>) showed significantly increased levels of IL10 in the hippocampus, although levels decreased by 12 months of age to values like those observed in WT mice (Fig. 8c). Hippocampal levels of the anti-inflammatory cytokine TGF $\beta$  were similar in 3- and 12-month-old WT mice, and were also like the levels observed in young transgenic mice. However, TGF $\beta$  was significantly reduced in the 12-month-old APP/PS1, SR-A<sup>-/-</sup> and APP/PS1/SR-A<sup>-/-</sup> mice (Fig. 8d). All changes were mild.

### 3.7. The absence of SR-A promotes an inflammatory environment with increased pro-inflammatory and reduced anti-inflammatory cytokines release

Production and release of cytokines into the extracellular medium by primary cultures of microglia (Fig. 9) and astrocytes (Fig. 10) was measured in basal conditions and after LPS stimulation. In basal conditions, microglia lacking functional SR-A (SR-A<sup>-/-</sup> and APP/PS1/SR-A<sup>-/-</sup>) released increased amounts of pro-

inflammatory cytokines IL1 $\beta$  and TNF $\alpha$  (Fig. 9a, b), but reduced amounts of the anti-inflammatory cytokines IL10 and TGF $\beta$  (Fig. 9c, d) compared with glial cells from WT and APP/PS1 mice.

After stimulation with LPS, SR-A<sup>-/-</sup> and APP/PS1/SR-A<sup>-/-</sup> microglia showed a reduced induction of the release of IL1 $\beta$  compared with WT and APP/PS1 cells (Fig. 9a). Furthermore, whereas LPS induced the release of TNF $\alpha$  by microglia of all genotypes (Fig. 9b), the induction was considerably reduced in SR-A<sup>-/-</sup> and APP/PS1/SR-A<sup>-/-</sup> microglia compared with the induction observed in microglia derived from WT and APP/PS1 mice. Remarkably, in response to LPS stimulation, release of IL10 by microglia increased 100-fold more in SR-A<sup>-/-</sup> and 180-fold more in APP/PS1/SR-A<sup>-/-</sup> than the induction observed in WT cells (Fig. 9c). No differences were found on LPS-induced release of TGF $\beta$  among the different genotypes (Fig. 9d).

Basal levels of IL1 $\beta$  were not significantly affected by the lack of SR-A, and LPS failed to increase the release of this cytokine in all genotypes (Fig. 10a). Like microglia, astrocytes lacking SR-A (SR-A<sup>-/-</sup> and APP/PS1/SR-A<sup>-/-</sup>) showed increased basal levels of TNF $\alpha$  (Fig. 10b). Induction by LPS in contrast, yield increase levels of TNF $\alpha$  in SR-A<sup>-/-</sup> and APP/PS1/SR-A<sup>-/-</sup> astrocytes (Fig. 10b). IL10 basal levels were similar for all genotypes. However, LPS induced a mild increase of IL10 release only in astrocytes deficient for SR-A, inducing significantly higher levels of IL10 in APP/PS1/SR-A<sup>-/-</sup> astrocytes than in WT or APP/PS1 astrocytes (Fig. 10c). Levels of the anti-inflammatory cytokine TGF $\beta$  were reduced in cells lacking SR-A (Fig. 10d). LPS did not affect the release of TGF $\beta$  for any of the genotypes (Fig. 10d).

### 3.8. Glial cell production of nitric oxide is impaired in the absence of SR-A

We quantified nitric oxide (NO) production in microglia and astrocytes in culture, to assess how the lack of SR-A affects NO

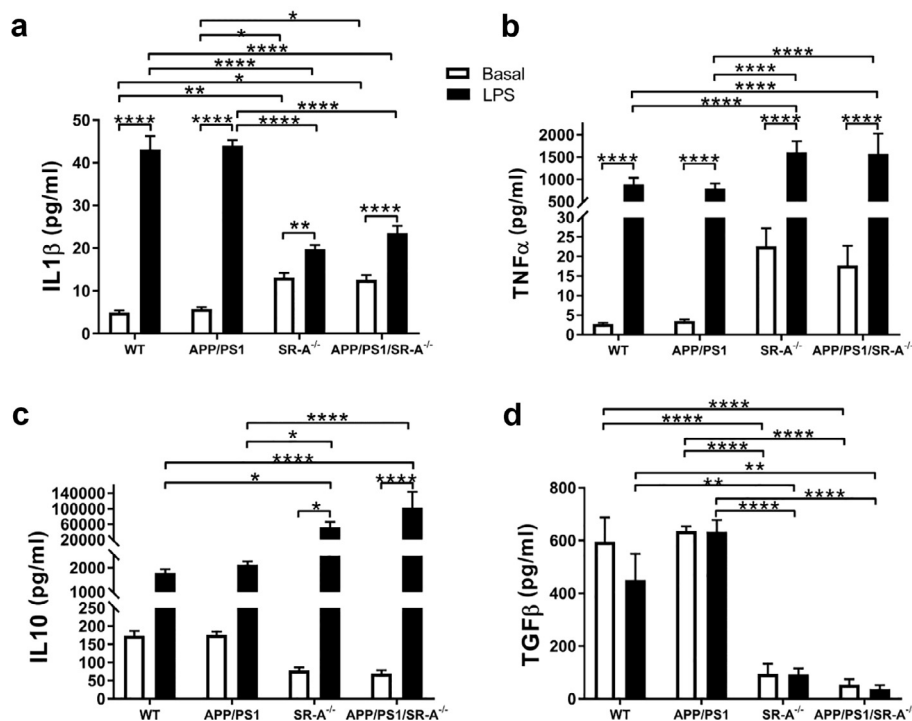


**Fig. 9.** Release of cytokines by microglia depends on the presence of SR-A. Inflammatory (a-b) and anti-inflammatory (c-d) cytokines released to the culture medium by neonatal microglia were assessed by ELISA. IL1 $\beta$  (a), TNF $\alpha$  (b), IL10 (c) and TGF $\beta$  levels (d) under basal conditions (white bars) and after 24 h of LPS treatment (black bars) are expressed as the mean  $\pm$  SEM. Two-way ANOVA revealed significant effect of genotype for IL1 $\beta$  ( $F(3,72) = 17.4, p < .0001$ ), TNF $\alpha$  ( $F(3, 41) = 18.96, p < .0001$ ), IL10 ( $F(3, 43) = 9.956, p < .0001$ ), and TGF $\beta$  ( $F(3, 31) = 47.11, p < .0001$ ). Significant effect on LPS-induction was obtained for IL1 $\beta$  ( $F(1,72) = 513.5, p < .0001$ ), TNF $\alpha$  ( $F(1, 41) = 545.1, p < .0001$ ), and IL10 ( $F(1, 43) = 30.83, p < .0001$ ), but not TGF $\beta$  ( $F(1, 31) = 0.921, p = 3.446$ ). \*, \*\*, \*\*\*, and \*\*\*\* indicate  $p < .05, p < .01, p < .001$ , and  $p < .0001$ , respectively for multiple comparisons with Bonferroni *post hoc* test. WT  $n = 9$ , APP/PS1  $n = 9$ , SR-A<sup>-/-</sup>  $n = 14$ , APP/PS1/SR-A<sup>-/-</sup>  $n = 11$  independent cultures.

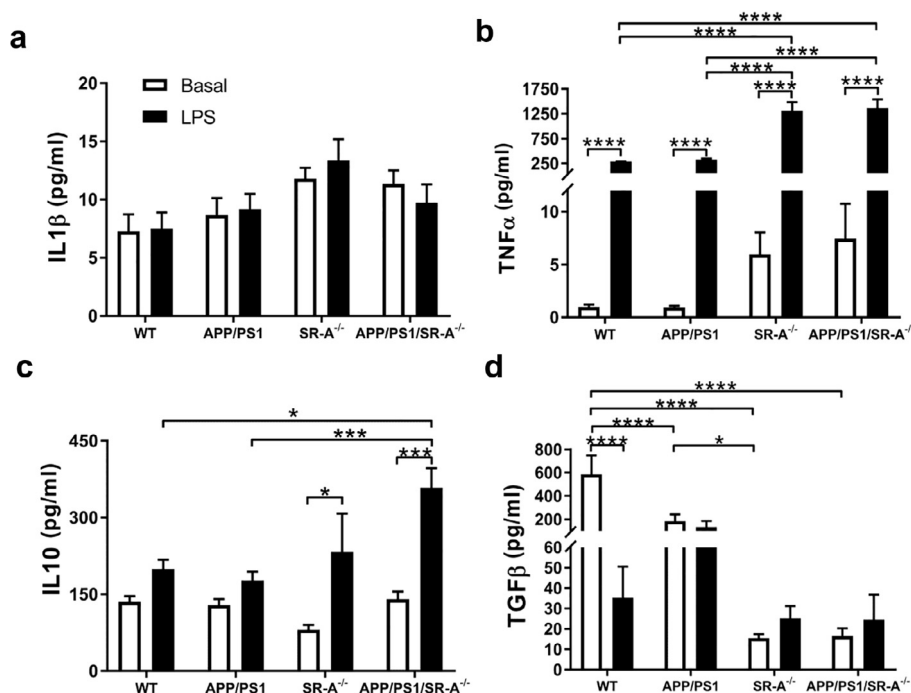


**Fig. 10.** Release of cytokines by astrocytes depends on the presence of SR-A. Inflammatory (a-b) and anti-inflammatory (c-d) cytokines released to the culture medium by neonatal astrocytes were assessed by ELISA. IL1 $\beta$  (a), TNF $\alpha$  (b), IL10 (c) and TGF $\beta$  levels (d) basal levels (white bars) and after 48 h of LPS treatment (black bars) are expressed as the mean  $\pm$  SEM. Two-way ANOVA analysis revealed significant effect of genotype for IL1 $\beta$  ( $F(3,142) = 3.899$ ,  $p < .0103$ ), TNF $\alpha$  ( $F(3,66) = 178.1$ ,  $p < 0.0001$ ), IL10 ( $F(3,56) = 4.553$ ,  $p < .0063$ ), and TGF $\beta$  ( $F(3,86) = 15.1$ ,  $p < .0001$ ). Significant effect on LPS-induction was also obtained for TNF $\alpha$  ( $F(1,66) = 1340$ ,  $p < .0001$ ), IL10 ( $F(1,56) = 31.34$ ,  $p < .0001$ ), and TGF $\beta$  ( $F(1,86) = 20.37$ ,  $p < .0001$ ), but not for IL1 $\beta$  ( $F(1,142) = 0.0239$ ,  $p = .8771$ ). \*, \*\*, \*\*\*, and \*\*\*\* indicate  $p < .05$ ,  $p < .01$ ,  $p < .001$ , and  $p < .0001$ , respectively for multiple comparisons with Bonferroni *post hoc* test. WT  $n = 9$ , APP/PS1  $n = 13$ , SR-A $^{-/-}$   $n = 24$ , APP/PS1/SR-A $^{-/-}$   $n = 18$  independent cultures.

production. NO release to the culture medium, as determined through its stable intermediary nitrite (NO $_2^-$ ), was measured under basal conditions and after LPS stimulation in culture (Fig. 11). In unstimulated conditions, microglia from WT, APP/PS1, SR-A $^{-/-}$  and APP/PS1/SR-A $^{-/-}$  mice showed similar levels of nitrite in culture (Fig. 11a). However, LPS stimulation induced a robust increase of nitrite release by WT and APP/PS1 microglia, but failed to increase nitrite release in microglia from SR-A $^{-/-}$  and APP/PS1/SR-A $^{-/-}$  mice (Fig. 11a). Astrocytes from SR-A $^{-/-}$  and APP/PS1/SR-A $^{-/-}$  mice showed slightly reduced basal extracellular levels of nitrite (Fig. 11b). Stimulation with LPS resulted in a 10-fold increase in NO release in WT astrocytes, but did not induce a significant increase in APP/PS1, SR-A $^{-/-}$  or APP/PS1/SR-A $^{-/-}$  (Fig. 11b).

### 3.9. Microglia lacking SR-A exhibit reduced oxidative response to LPS treatment

CM-H $_2$ DCF DA fluorescence was measured as an indirect assessment of the intracellular production of ROS by microglia and astrocytes in culture before and after LPS exposure (Fig. 12). In basal conditions, SR-A $^{-/-}$  microglia and astrocytes showed reduced intracellular ROS levels (Fig. 12a). After stimulation with LPS, WT and APP/PS1 microglia showed a 20% and 35% increase of intracellular ROS levels, respectively, whereas SR-A $^{-/-}$  and APP/PS1/SR-A $^{-/-}$  microglia were unable to induce intracellular ROS in response to LPS (Fig. 12a). Only a very mild induction of ROS was observed in astrocytes after treatment with LPS (Fig. 12b).

## 4. Discussion

Robust evidence show that A $\beta$  induces glial activation and neuroinflammation, potentiating neurodegeneration induced by A $\beta$

(Fernandez-Perez et al., 2016; Krabbe et al., 2013; Patel et al., 2005; Ramírez et al., 2008; Streit et al., 2009). A $\beta$  accumulation can result from reduced A $\beta$  clearance in AD brains (Domert et al., 2014; Jankowsky et al., 2005; Mawuenyega et al., 2010), being microglia the main cell involved in A $\beta$  removal (Daria et al., 2017; Efthymiou and Goate, 2017; Frautschy et al., 1998; Hickman et al., 2008; Krabbe et al., 2013; Paresce et al., 1996). Extracellular accumulation of A $\beta$  can be a consequence of the deterioration of glial function during aging, given that A $\beta$  is constantly being produced (Zhao et al., 2016), but the basal or the induced phagocytic capacity of microglia is reduced in older individuals (Mawuenyega et al., 2010; Njie et al., 2012; Tichauer et al., 2014). Moreover, reduced expression of SR-A involved in A $\beta$  phagocytosis (Hickman et al., 2008), promotes a vicious cycle that favors the accumulation of A $\beta$  plaques and the deregulation of the inflammatory activation of glia. As we have shown here, SR-A expression is reduced by A $\beta$  and the reduced expression of SR-A impairs the immune function of microglia and astrocytes (Murgas et al., 2014). Ours and previous results indicate that as individuals age, SR-A expression is reduced in the hippocampus, neuroinflammation increases (Lucin and Wyss-Coray, 2009), and A $\beta$  uptake became progressively impaired in the brain (Mawuenyega et al., 2010), favoring its extracellular accumulation, which in turn can further reduce SR-A expression (Hickman et al., 2008), potentiating impaired glial response, reduced life expectancy, and neurocognitive impairment (von Bernhardi et al., 2010). The glial alterations induced by reduced SR-A and A $\beta$  accumulation potentiate a pro-inflammatory environment that induce more neuroinflammation, favoring a positive loop for glial cell dysregulation and neurodegeneration (Fig. 13).

We have reported here that APP/PS1/SR-A $^{-/-}$  mice had a reduced life span, which has been reported in previous work using



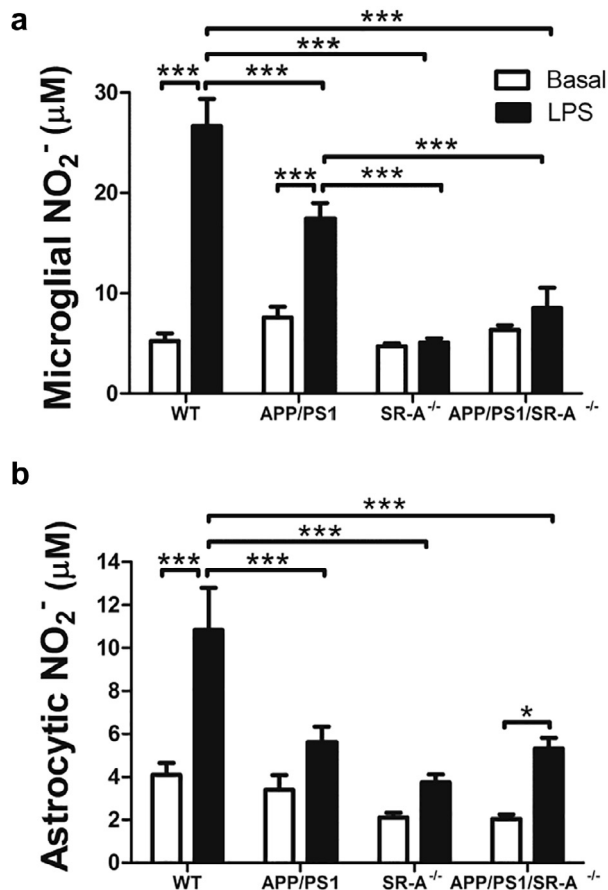


**Fig. 11.** Release of NO by astrocytes and microglia is affected by the presence of SR-A. Production of nitrite (NO<sub>2</sub><sup>-</sup>), a stable byproduct of NO, was assessed in microglia (a) and astrocytes (b) cultures. Nitrite release was assessed at basal conditions (white bars) and after LPS stimulation (black bars) for 48 h (microglia) or 72 h (astrocytes). Nitrite concentration (μM) is expressed as the mean ± SEM. Two-way ANOVA analysis showed a significant effect of LPS for microglia (df = 1, F ratio = 101.4, p < 0001) and astrocytes (df = 1, F ratio = 39.53, p < 0001) and significant effect of genotype for microglia (df = 3, F ratio = 36.02, p < 0001) and astrocytes (df = 1, F ratio = 14.59, p < 0001). \* and \*\* indicate p < .05 and p < .001 estimated with Bonferroni *post hoc* test. WT n = 10, APP/PS1 n = 10, SR-A<sup>-/-</sup> n = 16, APP/PS1/SR-A<sup>-/-</sup> n = 12 independent cultures.

an alternative AD mice model (Frenkel et al., 2013). It has been proposed that the concomitant effect of Aβ accumulation and lack of SR-A, which potentiates early death in the APP/PS1/SR-A<sup>-/-</sup> mice, may be related to a defective systemic macrophage function, a condition that could induce immune deficiency (Suzuki et al., 1997). Our analysis of the peripheral inflammatory state showed that young APP/PS1/SR-A<sup>-/-</sup> had elevated plasma levels of IL1β and TNFα, indicative of an early systemic inflammation. Also, adult mice lacking SR-A showed increased plasma levels of both cytokines. The data suggests that Aβ accumulation and SR-A absence inflammatory outcome that could be at least partially responsible of the high mortality rate observed in these mice. Although there are not profound changes in peripheral immunity in AD patients, there are systemic inflammatory changes even at early stages of AD (De Luigi et al., 2002; Holmes et al., 2009; Kim et al., 2011; O'Banion, 2014; Lai et al., 2017).

Analysis of the behavioral performance showed in the 6ARWM test, which mainly evaluates working memory (Hyde et al., 1998), that APP/PS1/SR-A<sup>-/-</sup> mice showed a significantly higher latency time at the second day of test, in which the animals present the worst behavioral performance. Test evaluating spatial memory (Vorhees and Williams, 2006), showed significant differences in

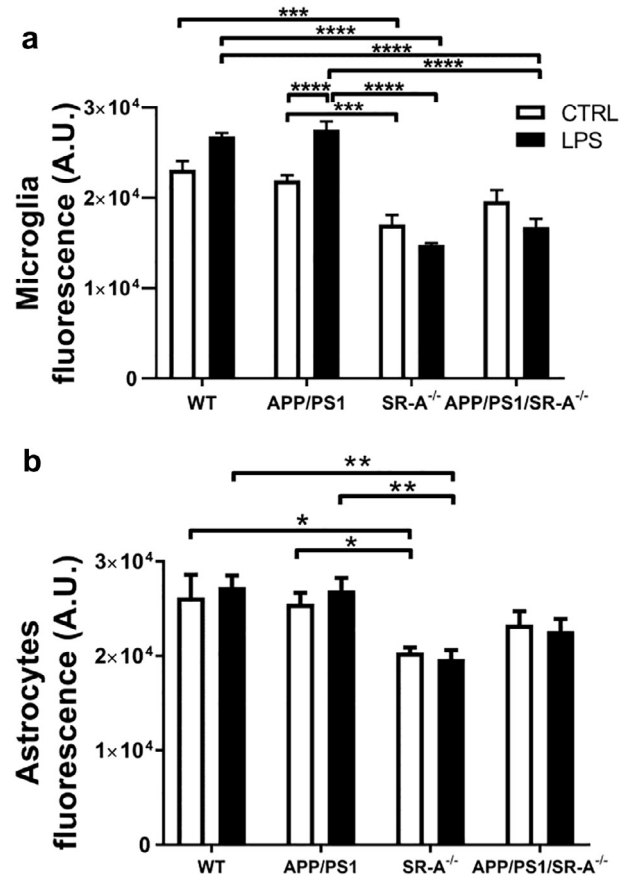


**Fig. 12.** ROS production by glial cells is reduced in the absence of SR-A. Microglia (a) and astrocytes (b) in primary cell cultures were incubated with the fluorescent probe CM-H<sub>2</sub>DCF DA to measure the production of intracellular ROS in unstimulated conditions (white bars) and after LPS stimulation (black bars). Basal levels of intracellular ROS in microglia (a) and astrocytes (b) are expressed in arbitrary units (A.U.) as the mean ± SEM fluorescence emitted at 530 nm. Two-way ANOVA with repeated measures revealed significant genotype effect for microglia (F (3, 19) = 49, p < .0001) and for astrocytes (F (3, 15) = 8.98, p = .0012) and no global effect of LPS treatment for microglia (F (1,19) = 3.229, p = .0883) and for astrocytes (F (1,15) = 0.1508, p = .7032), but there is induced response to LPS in APP/PS1 microglia (\*, \*\*, \*\*\*, and \*\*\*\* indicate p < .05, p < .01, p < .001, and p < .00001, respectively (Bonferroni *post hoc* test); the number for each experiment in triplicate is indicated under each bar. WT n = 5, APP/PS1 n = 9, SR-A<sup>-/-</sup> n = 5, APP/PS1/SR-A<sup>-/-</sup> n = 4 independent experiments in triplicate.

latency times only in the first day. It has been previously shown that mice do not exhibit alterations in spatial memory at 9 months of age (Holcomb et al., 1999) and not at 12 months. However, we evaluated the mice at 9 months, instead of 12 months (Maei et al., 2009), because of the high mortality of the APP/PS1/SR-A<sup>-/-</sup> mice.

The deleterious effect over working memory observed in APP/PS1/SR-A<sup>-/-</sup> mice could be related to the fact that the earliest damage in AD mice models occurs in areas of the hippocampus interacting with the prefrontal cortex (Floresco et al., 1997; Laroche et al., 2000). This could depend on the high density of microglia in the subiculum of the hippocampus that is directly interconnected with the prefrontal cortex (Laroche et al., 2000; DiPatre and Gelman, 1997).

The absence of SR-A increased the accumulation of Aβ in the hippocampus, which is consistent with previous reports (Frenkel et al., 2013). Even though the number of microglia associated to each plaque was similar, there was a higher density of CD68-positive cells in the hippocampus of APP/PS1/SR-A<sup>-/-</sup> compared to APP/PS1 mice. CD68 is a lysosomal phagocytic activation marker

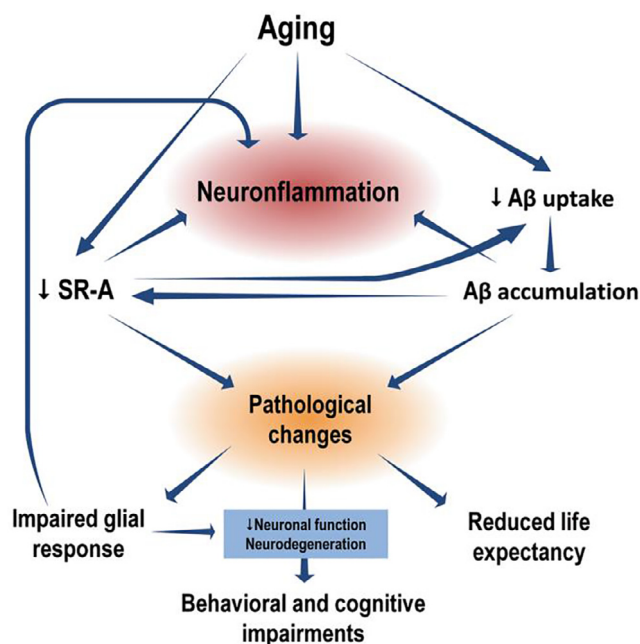


**Fig. 13.** Reduced SR-A expression potentiate neuroinflammation. It has been previously shown that aging induces neuroinflammation and facilitates A $\beta$  accumulation by reducing A $\beta$  uptake and increasing their aggregation. We show that aging reduces SR-A expression in the hippocampus, reducing A $\beta$  uptake, and increased A $\beta$  accumulation further reduces SR-A expression. Decreased SR-A expression in concomitancy with A $\beta$  accumulation produce pathological changes, including reduced life expectancy, impaired glial response, and neurocognitive impairment, possibly due to reduced neuronal function and neurodegeneration induced by the neuroinflammatory environment generated by the impaired glial response. In addition, the altered immune response mediated by impaired function of glial cells contributes to more neuroinflammation, establishing a deleterious feedback loop for the development of memory impairment, promoting AD progression (Heppner et al., 2015; Liu et al., 2012; Mawuenyega et al., 2010; Njie et al., 2012; Tichauer et al., 2014; von Bernhardi et al., 2010).

and its expression is gradually increased in AD animal models as the accumulation of A $\beta$  plaques increases (Matsumura et al., 2015), which suggests that increased CD68 expression could be a consequence of A $\beta$  accumulation.

The increased A $\beta$  levels observed in the hippocampus could be due at least partially to the fact that the absence of SR-A reduces the phagocytosis of A $\beta$  both *in vitro* and *ex vivo*, as it has been previously reported (Frenkel et al., 2013; Lifshitz et al., 2013). SR-A is one of the most important for A $\beta$  phagocytosis, but multiple scavenger receptors participate in A $\beta$  clearance (Chung et al., 2001). Microglia from WT and APP/PS1 mice showed an age-related reduction in A $\beta$  uptake, strengthening the notion that the phagocytic capacity is reduced in aging (Mawuenyega et al., 2010; Njie et al., 2012).

It is especially relevant that microglia lacking SR-A had basal levels of pro-inflammatory cytokines which were up to 6-fold higher than those of cells with functional SR-A. Neuroinflammation is pro-amyloidogenic, increasing APP expression, amyloidogenic processing of APP increasing A $\beta$  levels, and favoring A $\beta$  aggregation (Blasko et al., 1999; Brugg et al., 1995; Buxbaum et al., 1992; Herbst-Robinson et al., 2015; Sastre et al., 2003; Wyss-Coray and Mucke, 2002), all of which will be potentiated by the reduced uptake of A $\beta$  in the absence of SR-A. Microglia lacking SR-A had an increased basal release of IL1 $\beta$ , which has been associated with neurodegeneration (Allan and Rothwell, 2001; Yamasaki et al., 1995). In the hippocampus, IL1 $\beta$  level was specially increased in aged SR-A $^{-/-}$  mice, significantly higher than the increment observed during aging (Sparkman and Johnson, 2008). However,

the induction of IL1 $\beta$  after LPS stimulation was decreased. Microglia and astrocytes from mice lacking SR-A had increased basal levels of TNF $\alpha$ , which can induce apoptosis (Downen et al., 1999) and also participates in the regulation of the immune system (Aggarwal, 2003). Thus, microglia lacking SR-A appears to be over activated in basal conditions but also respond abnormally to inflammatory agents. The impairment of SR-A $^{-/-}$  glia to respond to LPS is especially striking considering that toll like receptors (TLRs) especially TLR4 and TLR2, appear to be the most sensitive receptors for LPS, acting together with other binding proteins like CD14 and LBP (Fenton and Golenbock, 1998; Takeuchi et al., 1999; Yang et al., 1998), indicating that in addition to its scavenger function, SR-A is also capable of regulating the inflammatory response of other receptors. In the absence of SR-A, microglia could send danger-associated signals under non-stimulated conditions, and have an impaired defensive role by losing its capability to respond when exposed to pathogenic agents (Kettenmann et al., 2013), in support to our hypothesis that the development of cognitive impairment and later AD could be due to glial dysregulation (von Bernhardi, 2007), and not the accumulation of A $\beta$  plaques (Dickson, 1997; Duyckaerts et al., 1998; Gordon et al., 2001).

Microglia devoid of SR-A had low basal levels of IL10, but levels rose above 100-fold after LPS-stimulation, compared with the normal 10-fold increase observed in WT and APP/PS1 microglia. A similar response was observed in astrocytes, although LPS-induced cytokine levels were lower than those observed in microglia. Surprisingly, IL10 was significantly elevated in the hippocampus of 3-month-old APP/PS1/SR-A $^{-/-}$  mice. IL10 promotes neuroprotection and modulates the expression of pro-inflammatory cytokines (Knobloch and Faden, 1998; Spera et al., 1998). Increased levels of regulatory cytokines could be established to compensate for the inflammatory environment in the hippocampus at early age. However, high levels of IL10 have deleterious effects over A $\beta$  proteostasis and AD pathophysiology (Chakrabarty et al., 2015; Guillot-Sestier et al., 2015). Thus, high levels of IL10 in APP/PS1/SR-A $^{-/-}$  young mice could promote glial dysfunction.

Glial cells exert an intricate crosstalk that regulates their immune response, in which astrocytes generally attenuates microglial cytotoxic activation (Orellana et al., 2013; Roth et al., 2005; Tichauer et al., 2007; von Bernhardi and Eugenin, 2004). The cytokine profile observed in both primary glial cell cultures and the hippocampus indicated that SR-A participates in the modulation of the inflammatory response of microglia and astrocytes. Production of NO and ROS was assessed because they constitute a first line of defense (Babior, 2000; Liu et al., 2002), and NO and ROS production by glia is closely correlated with neuronal damage (Block and Hong, 2005; Jeohn et al., 2000). Basal production of NO by astrocytes was reduced in the absence of SR-A. LPS induced a significant increase in the production of NO and ROS in WT and APP/PS1 microglia (Martha and Sean, 1992; Pawate et al., 2004; Ramírez et al., 2008), but the induction was abolished in cells lacking SR-A, indicating a defective microglial response to inflammatory stimulus. These changes in astrocytes immune response could redound into microglial dysregulation, since astrocytes are the main attenuators for microglia-mediated cytotoxicity (Orellana et al., 2013; von Bernhardi and Eugenin, 2004).

#### 4.1. Conclusions

Our results lead us to conclude that SR-A regulates the inflammatory state of microglia and astrocytes, being not only involved in A $\beta$  uptake as has been previously shown (Frenkel et al., 2013; Lifshitz et al., 2013), but also shaping the activation of glial cells. Given the increased importance of neuroinflammation, the APP/PS1/SR-A $^{-/-}$  mice model illustrates the significance of SR-A as modulator of the brain inflammatory processes.

This is especially relevant when taking into account that A $\beta$  accumulation is associated with a reduction of SR-A expression (Hickman et al., 2008), leading to the establishment of an increasingly inflammatory environment, as observed in the APP/PS1/SR-A<sup>-/-</sup>. Thus, the APP/PS1/SR-A<sup>-/-</sup> mice model could emulate some effects of aging, given that A $\beta$  is constantly produced in the brain (Mawuenyega et al., 2010; Zhao et al., 2016). Because there is scarce information regarding many of the molecular changes induced early in the brain of AD patients, the study of potential changes in SR-A expression associated with aging and the genesis and progression of AD in humans, would enlighten the field about one of the potential mechanisms leading to LOAD.

### Conflict of interests

None of the authors declare any conflict of interest.

### Acknowledgments

This study was supported by the grant 1131025 and 1171645 of the Fondo Nacional de Desarrollo Científico y Tecnológico (FONDECYT) from CONICYT (RvB), 1171434 (JE) and the fellowship 21120013 of the Comisión Nacional de Investigación Científica y Tecnológica (CONICYT) (FC). We acknowledge the “Proyecto Mecespup PUC0815 – Equipamiento Científico Mayor de la Pontificia Universidad Católica de Chile” for the access to the microscopy facility and the stereology system. We thank Mrs. Ximena Verges for excellent help with the confocal microscopy, and Dr. Tatsuhiko Kodama (Research Center for Advanced Science and Technology, University of Tokyo, Japan) for facilitating the SR-A<sup>-/-</sup> mice (129/ICR background).

### Appendix A. Supplementary data

Supplementary data associated with this article can be found, in the online version, at <https://doi.org/10.1016/j.bbi.2017.12.007>.

### References

- Aggarwal, B.B., 2003. Signalling pathways of the TNF superfamily: a double-edged sword. *Nat. Rev. Immunol.* 3, 745–756.
- Allan, S., Rothwell, N., 2001. Cytokines and acute neurodegeneration. *Nat. Rev. Neurosci.* 2, 734–744.
- Babior, B., 2000. Phagocytes and oxidative stress. *Am. J. Med.* 109, 33–44.
- Blasko, I., Marx, F., Steiner, E., Hartmann, T., Grubeck-Loebenstein, B., 1999. TNF $\alpha$  plus IFN $\gamma$  induce the production of Alzheimer beta-amyloid peptides and decrease the secretion of APPs. *FASEB J.: Off. Publ. Fed. Am. Soc. Exp. Biol.* 13, 63–68.
- Block, M., Hong, J.-S., 2005. Microglia and inflammation-mediated neurodegeneration: multiple triggers with a common mechanism. *Progress Neurobiol.* 76, 77–98.
- Bronstein, R., Torres, L., Nissen, J., Tsirka, S., 2013. Culturing microglia from the neonatal and adult central nervous system. *J. Visualized Exp.*
- Brugg, B., Dubreuil, Y.L., Huber, G., Wollman, E.E., Delhaye-Bouchaud, N., Mariani, J., 1995. Inflammatory processes induce beta-amyloid precursor protein changes in mouse brain. *Proc. Natl. Acad. Sci. U.S.A.* 92, 3032–3035.
- Buxbaum, J.D., Oishi, M., Chen, H.L., Pinkas-Kramarski, R., Jaffe, E.A., Gandy, S.E., Greengard, P., 1992. Cholinergic agonists and interleukin 1 regulate processing and secretion of the Alzheimer beta/A4 amyloid protein precursor. *Proc. Natl. Acad. Sci. U.S.A.* 89, 10075–10078.
- Cardona, A., Huang, D., Sasse, M., Ransohoff, R., 2006. Isolation of murine microglial cells for RNA analysis or flow cytometry. *Nat. Protocols* 1, 1947–1951.
- Cornejo, F., von Bernhard, R., 2013. Role of scavenger receptors in glia-mediated neuroinflammatory response associated with Alzheimer's disease. *Mediators Inflammation* 2013, 895651.
- Chakrabarty, P., Li, A., Ceballos-Diaz, C., Eddy, J.A., Funk, C.C., Moore, B., DiNunno, N., Rosario, A.M., Cruz, P.E., Verbeeck, C., Sacino, A., Nix, S., Janus, C., Price, N.D., Das, P., Golde, T.E., 2015. IL-10 alters immunoproteostasis in APP mice, increasing plaque burden and worsening cognitive behavior. *Neuron* 85, 519–533.
- Chung, H., Brazil, M., Irizarry, M., Hyman, B., Maxfield, F., 2001. Uptake of fibrillar beta-amyloid by microglia isolated from MSR-A (type I and type II) knockout mice. *Neuroreport* 12, 1151–1154.
- Daria, A., Colombo, A., Llovera, G., Hampel, H., Willem, M., Liesz, A., Haass, C., Tahirovic, S., 2017. Young microglia restore amyloid plaque clearance of aged microglia. *EMBO J.* 36, 583–603.
- De Luigi, A., Pizzimenti, S., Quadri, P., Lucca, U., Tettamanti, M., Fragiaco, C., De Simoni, M.G., 2002. Peripheral inflammatory response in Alzheimer's disease and multi-infarct dementia. *Neurobiol. Dis.* 11, 308–314.
- Dickson, D.W., 1997. The pathogenesis of senile plaques. *J. Neurobiol. Exp. Neurol.* 56, 321–339.
- DiPatre, P.L., Gelman, B.B., 1997. Microglial cell activation in aging and Alzheimer disease: partial linkage with neurofibrillary tangle burden in the hippocampus. *J. Neurobiol. Exp. Neurol.* 56, 143–149.
- Domert, J., Rao, S.B., Agholme, L., Brorsson, A.-C.C., Marcusson, J., Hallbeck, M., Nath, S., 2014. Spreading of amyloid- $\beta$  peptides via neuritic cell-to-cell transfer is dependent on insufficient cellular clearance. *Neurobiol. Dis.* 65, 82–92.
- Downen, M., Amaral, T., Hua, L., Zhao, M., Lee, S., 1999. Neuronal death in cytokine-activated primary human brain cell culture: role of tumor necrosis factor- $\alpha$ . *Glia* 28, 114–127.
- Duyckaerts, C., Colle, M.A., Dessi, F., Grignon, Y., Piette, F., Hauw, J.J., 1998. The progression of the lesions in Alzheimer disease: insights from a prospective clinicopathological study. *J. Neural Trans. Suppl.* 53, 119–126.
- Efthymiou, A.G., Goate, A.M., 2017. Late onset Alzheimer's disease genetics implicates microglial pathways in disease risk. *Mol. Neurodegeneration* 12, 43.
- El Khoury, J., Hickman, S., Thomas, C., Loike, J., Silverstein, S., 1998. Microglia, scavenger receptors, and the pathogenesis of Alzheimer's disease. *Neurobiol. Aging* 19, 4.
- Fenton, M.J., Golenbock, D.T., 1998. LPS-binding proteins and receptors. *J. Leukocyte Biol.* 64, 25–32.
- Fernandez-Perez, E., Peters, C., Aguayo, L., 2016. Membrane damage induced by amyloid beta and a potential link with neuroinflammation. *Curr. Pharm. Des.* 22, 1295–1304.
- Floresco, S.B., Seamans, J.K., Phillips, A.G., 1997. Selective roles for hippocampal, prefrontal cortical, and ventral striatal circuits in radial-arm maze tasks with or without a delay. *J. Neurosci.* 17, 1880–1890.
- Franceschi, C., Capri, M., Monti, D., Giunta, S., Olivieri, F., Sevini, F., Panourgia, M., Invidia, L., Celani, L., Scurti, M., Cevenini, E., Castellani, G., Salvio, S., 2007. Inflammaging and anti-inflammaging: a systemic perspective on aging and longevity emerged from studies in humans. *Mech. Ageing Dev.* 128, 92–105.
- Frank, M., Barrientos, R., Watkins, L., Maier, S., 2010. Aging sensitizes rapidly isolated hippocampal microglia to LPS ex vivo. *J. Neuroimmunology* 226, 181–184.
- Frautschy, S.A., Yang, F., Irizarry, M., Hyman, B., Saido, T.C., Hsiao, K., Cole, G.M., 1998. Microglial response to amyloid plaques in APPsw transgenic mice. *Am. J. Pathol.* 152, 307–317.
- Frenkel, D., Wilkinson, K., Zhao, L., Hickman, S., Means, T., Puckett, L., Farfara, D., Kingery, N., Weiner, H., El Khoury, J., 2013. Scara1 deficiency impairs clearance of soluble amyloid- $\beta$  by mononuclear phagocytes and accelerates Alzheimer's-like disease progression. *Nat. Commun.* 4, 2030.
- Gallina, P., Scollato, A., Conti, R., Di Lorenzo, N., Porfirio, B., 2015. Abeta clearance, “hub” of multiple deficiencies leading to Alzheimer disease. *Front Aging Neurosci.* 7, 200.
- Giulian, D., Baker, T.J., 1986. Characterization of ameboid microglia isolated from developing mammalian brain. *J. Neurosci.* 6, 2163–2178.
- Godoy, B., Murgas, P., Tichauer, J., Von Bernhard, R., 2012. Scavenger receptor class A ligands induce secretion of IL1 $\beta$  and exert a modulatory effect on the inflammatory activation of astrocytes in culture. *J. Neuroimmunology* 251, 6–13.
- Golub, V.M., Brewer, J., Wu, X., Kuruba, R., Short, J., Manchi, M., Swonke, M., Younus, I., Reddy, D.S., 2015. Neurostereology protocol for unbiased quantification of neuronal injury and neurodegeneration. *Front. Aging Neurosci.* 7, 196.
- Gordon, M.N., King, D.L., Diamond, D.M., Jantzen, P.T., Boyett, K.V., Hope, C.E., Hatcher, J.M., DiCarlo, G., Gottschall, W.P., Morgan, D., Arendash, G.W., 2001. Correlation between cognitive deficits and Abeta deposits in transgenic APP +PS1 mice. *Neurobiol. Aging* 22, 377–385.
- Guillot-Sestier, M.V., Doty, K.R., Gate, D., Rodriguez Jr., J., Leung, B.P., Rezai-Zadeh, K., Town, T., 2015. IL10 deficiency rebalances innate immunity to mitigate Alzheimer-like pathology. *Neuron* 85, 534–548.
- Heppner, F.L., Ransohoff, R.M., Becher, B., 2015. Immune attack: the role of inflammation in Alzheimer disease. *Nat. Rev. Neurosci.* 16, 358–372.
- Herbst-Robinson, K.J., Liu, L., James, M., Yao, Y., Xie, S.X., Brunden, K.R., 2015. Inflammatory eicosanoids increase amyloid precursor protein expression via activation of multiple neuronal receptors. *Sci. Rep.* 5, 18286.
- Hickman, S., Allison, E., El Khoury, J., 2008. Microglial dysfunction and defective beta-amyloid clearance pathways in aging Alzheimer's disease mice. *J. Neurosci.: Off. J. Soc. Neurosci.* 28, 8354–8360.
- Holcomb, L.A., Gordon, M.N., Jantzen, P., Hsiao, K., Duff, K., Morgan, D., 1999. Behavioral changes in transgenic mice expressing both amyloid precursor protein and presenilin-1 mutations: lack of association with amyloid deposits. *Behav. Genet.* 29, 177–185.
- Holmes, C., Cunningham, C., Zotova, E., Woolford, J., Dean, C., Kerr, S., Culliford, D., Perry, V.H., 2009. Systemic inflammation and disease progression in Alzheimer disease. *Neurology* 73 (10), 768–774.
- Hou, J., Riise, J., Pakkenberg, B., 2012. Application of immunohistochemistry in stereology for quantitative assessment of neural cell populations illustrated in the Göttingen minipig. *PLoS One* 7, e43556.
- Hyde, L.A., Hoplight, B.J., Denenberg, V.H., 1998. Water version of the radial-arm maze: learning in three inbred strains of mice. *Brain Res.* 785, 236–244.



- Jankowsky, J.L., Slunt, H.H., Gonzales, V., Savonenko, A.V., Wen, J.C., Jenkins, N.A., Copeland, N.G., Younkin, L.H., Lester, H.A., Younkin, S.G., Borchelt, D.R., 2005. Persistent amyloidosis following suppression of Abeta production in a transgenic model of Alzheimer disease. *PLoS Med.* 2.
- Jeohn, G., Kim, W., Hong, J., 2000. Time dependency of the action of nitric oxide in lipopolysaccharide-interferon-gamma-induced neuronal cell death in murine primary neuron-glia co-cultures. *Brain Res.* 880, 173–177.
- Kettenmann, H., Kirchhoff, F., Verkhratsky, A., 2013. Microglia: new roles for the synaptic stripper. *Neuron.* 77, 10–18.
- Kim, S.M., Song, J., Kim, S., Han, C., Park, M.H., Koh, Y., Jo, S.A., Kim, Y.Y., 2011. Identification of peripheral inflammatory markers between normal control and Alzheimer's disease. *BMC Neurol.* 11, 51. <https://doi.org/10.1186/1471-2377-11-51>.
- Knobloch, S., Faden, A., 1998. Interleukin-10 improves outcome and alters proinflammatory cytokine expression after experimental traumatic brain injury. *Exp. Neurol.* 153, 143–151.
- Krabbe, G., Halle, A., Matyash, V., Rinnenthal, J., Eom, G., Bernhardt, U., Miller, K., Prokop, S., Kettenmann, H., Heppner, F., 2013. Functional impairment of microglia coincides with Beta-amyloid deposition in mice with Alzheimer-like pathology. *PLoS One* 8.
- Lai, K.S.P., Liu, C.S., Rau, A., Lanctôt, K.L., Köhler, C.A., Pakosh, M., Carvalho, A.F., Herrmann, N., 2017. Peripheral inflammatory markers in Alzheimer's disease: a systematic review and meta-analysis of 175 studies. *J. Neurol. Neurosurg. Psychiatry.* 88 (10), 876–882.
- Laroche, S., Davis, S., Jay, T.M., 2000. Plasticity at hippocampal to prefrontal cortex synapses: dual roles in working memory and consolidation. *Hippocampus* 10, 438–446.
- Lifshitz, V., Weiss, R., Levy, H., Frenkel, D., 2013. Scavenger receptor A deficiency accelerates cerebrovascular amyloidosis in an animal model. *J. Mol. Neurosci.: MN* 50, 198–203.
- Liu, B., Gao, H.-M., Wang, J.-Y., Jeohn, G.-H., Cooper, C., Hong, J.-S., 2002. Role of nitric oxide in inflammation-mediated neurodegeneration. *Ann. N. Y. Acad. Sci.* 962, 318–331.
- Liu, X., Wu, Z., Hayashi, Y., Nakanishi, H., 2012. Age-dependent neuroinflammatory responses and deficits in long-term potentiation in the hippocampus during systemic inflammation. *Neuroscience* 216, 133–142.
- Lucin, K., Wyss-Coray, T., 2009. Immune activation in brain aging and neurodegeneration: too much or too little? *Neuron* 64, 110–122.
- Lue, L., Rydel, R., Brigham, E., Yang, L., Hampel, H., Murphy, G., Brachova, L., Yan, S., Walker, D., Shen, Y., Rogers, J., 2001. Inflammatory repertoire of Alzheimer's disease and nondemented elderly microglia in vitro. *Glia* 35, 72–79.
- Maei, H.R., Zaslavsky, K., Teixeira, C.M., Frankland, P.W., 2009. What is the most sensitive measure of water maze probe test performance? *Front. Integr. Neurosci.* 3, 4.
- Martha, L.S., Sean, M., 1992. Induction of nitric oxide synthase in Glial cells. *J. Neurochem.* 59.
- Matsumura, A., Suzuki, S., Iwahara, N., Hisahara, S., Kawamata, J., Suzuki, H., Yamauchi, A., Takata, K., Kitamura, Y., Shimohama, S., 2015. Temporal changes of CD68 and  $\alpha 7$  nicotinic acetylcholine receptor expression in microglia in Alzheimer's disease-like mouse models. *J. Alzheimer's Dis.: JAD* 44, 409–423.
- Mawuenyega, K.G., Sigurdson, W., Ovod, V., Munsell, L., Kasten, T., Morris, J.C., Yarasheski, K.E., Bateman, R.J., 2010. Decreased clearance of CNS beta-amyloid in Alzheimer's disease. *Science (New York, N.Y.)* 330, 1774.
- McIntee, F.L., Giannoni, P., Blais, S., Sommer, G., Neubert, T.A., Rostagno, A., Ghiso, J., 2016. In vivo differential brain clearance and catabolism of monomeric and oligomeric Alzheimer's A beta protein. *Front. Aging Neurosci.* 8, 223.
- Medeiros, R., LaFerla, F., 2013. Astrocytes: conductors of the Alzheimer disease neuroinflammatory symphony. *Exp. Neurol.* 239, 133–138.
- Mosher, K., Wyss-Coray, T., 2014. Microglial dysfunction in brain aging and Alzheimer's disease. *Biochem. Pharmacol.* 88, 594–604.
- Murgas, P., Cornejo, F., Merino, G., von Bernhardi, R., 2014. SR-A regulates the inflammatory activation of astrocytes. *Neurotoxic. Res.* 25, 68–80.
- Njie, E., Boelen, E., Stassen, F., Steinbusch, H., Borchelt, D., Streit, W., 2012. Ex vivo cultures of microglia from young and aged rodent brain reveal age-related changes in microglial function. *Neurobiol. Aging* 33, 1950–1912.
- O'Banion, M.K., 2014. Does peripheral inflammation contribute to Alzheimer disease? Evidence from animal models. *Neurology.* 83 (6), 480–481.
- Olabarria, M., Noristani, H., Verkhratsky, A., Rodríguez, J., 2010. Concomitant astroglial atrophy and astrogliosis in a triple transgenic animal model of Alzheimer's disease. *Glia* 58, 831–838.
- Orellana, J., Montero, T., von Bernhardi, R., 2013. Astrocytes inhibit nitric oxide-dependent Ca(2+) dynamics in activated microglia: involvement of ATP released via pannexin 1 channels. *Glia* 61, 2023–2037.
- Paresce, D.M., Ghosh, R.N., Maxfield, F.R., 1996. Microglial cells internalize aggregates of the Alzheimer's disease amyloid beta-protein via a scavenger receptor. *Neuron* 17, 553–565.
- Patel, N., Paris, D., Mathura, V., Quadros, A., Crawford, F., Mullan, M., 2005. Inflammatory cytokine levels correlate with amyloid load in transgenic mouse models of Alzheimer's disease. *J. Neuroinflammation* 2, 9.
- Patterson, B.W., Elbert, D.L., Mawuenyega, K.G., Kasten, T., Ovod, V., Ma, S., Xiong, C., Chott, R., Yarasheski, K., Sigurdson, W., Zhang, L., Goate, A., Benzinger, T., Morris, J.C., Holtzman, D., Bateman, R.J., 2015. Age and amyloid effects on human central nervous system amyloid-beta kinetics. *Ann. Neurol.* 78, 439–453.
- Pawate, S., Shen, Q., Fan, F., Bhat, N., 2004. Redox regulation of glial inflammatory response to lipopolysaccharide and interferon-gamma. *J. Neurosci. Res.* 77, 540–551.
- Pfeiffer, S., Gorren, A.C., Schmidt, K., Werner, E.R., Hansert, B., Bohle, D.S., Mayer, B., 1997. Metabolic fate of peroxynitrite in aqueous solution. Reaction with nitric oxide and pH-dependent decomposition to nitrite and oxygen in a 2:1 stoichiometry. *J. Biol. Chem.* 272, 3465–3470.
- Ramírez, G., Rey, S., von Bernhardi, R., 2008. Proinflammatory stimuli are needed for induction of microglial cell-mediated AbetaPP<sub>(244-C)</sub> and Abeta-neurotoxicity in hippocampal cultures. *J. Alzheimer's Dis.: JAD* 15, 45–59.
- Rodríguez, J., Butt, A., Gardenal, E., Parpura, V., Verkhratsky, A., 2016. Complex and differential glial responses in Alzheimer's disease and ageing. *Curr. Alzheimer Res.* 13, 343–358.
- Roth, A., Ramírez, G., Alarcón, R., Von Bernhardi, R., 2005. Oligodendrocytes damage in Alzheimer's disease: beta amyloid toxicity and inflammation. *Biol. Res.* 38, 381–387.
- Rozovsky, I., Finch, C., Morgan, T., 1998. Age-related activation of microglia and astrocytes: in vitro studies show persistent phenotypes of aging, increased proliferation, and resistance to down-regulation. *Neurobiol. Aging* 19, 97–103.
- Sastre, M., Dewachter, I., Landreth, G.E., Willson, T.M., Klockgether, T., van Leuven, F., Heneka, M.T., 2003. Nonsteroidal anti-inflammatory drugs and peroxisome proliferator-activated receptor-gamma agonists modulate immunostimulated processing of amyloid precursor protein through regulation of beta-secretase. *J. Neurosci.* 23, 9796–9804.
- Savonenko, A., Xu, G.M., Melnikova, T., Morton, J.L., Gonzales, V., Wong, M.P., Price, D.L., Tang, F., Markowska, A.L., Borchelt, D.R., 2005. Episodic-like memory deficits in the APP<sup>swe</sup>/PS1<sup>dE9</sup> mouse model of Alzheimer's disease: relationships to beta-amyloid deposition and neurotransmitter abnormalities. *Neurobiol. Dis.* 18, 602–617.
- Sparkman, N., Johnson, R., 2008. Neuroinflammation associated with aging sensitizes the brain to the effects of infection or stress. *Neuroimmunomodulation* 15, 323–330.
- Spera, P., Ellison, J., Feuerstein, G., Barone, F., 1998. IL-10 reduces rat brain injury following focal stroke. *Neurosci. Lett.* 251, 189–192.
- Streit, W., Braak, H., Xue, Q.-S., Bechmann, I., 2009. Dystrophic (senescent) rather than activated microglial cells are associated with tau pathology and likely precede neurodegeneration in Alzheimer's disease. *Acta neuropathologica* 118, 475–485.
- Suzuki, H., Kurihara, Y., Takeya, M., Kamada, N., Kataoka, M., Jishage, K., Ueda, O., Sakaguchi, H., Higashi, T., Suzuki, T., Takashima, Y., Kawabe, Y., Cynshi, O., Wada, Y., Honda, M., Kurihara, H., Aburatani, H., Doi, T., Matsumoto, A., Azuma, S., Noda, T., Toyoda, Y., Itakura, H., Yazaki, Y., Kodama, T., 1997. A role for macrophage scavenger receptors in atherosclerosis and susceptibility to infection. *Nature* 386, 292–296.
- Takeuchi, O., Hoshino, K., Kawai, T., Sanjo, H., Takada, H., Ogawa, T., Takeda, K., Akira, S., 1999. Differential roles of TLR2 and TLR4 in recognition of gram-negative and gram-positive bacterial cell wall components. *Immunity* 11, 443–451.
- Tichauer, J., Flores, B., Soler, B., Eugenín-von Bernhardi, L., Ramírez, G., von Bernhardi, R., 2014. Age-dependent changes on TGFβ1 Smad3 pathway modify the pattern of microglial cell activation. *Brain, Behav., Immun.* 37, 187–196.
- Tichauer, J., Saud, K., von Bernhardi, R., 2007. Modulation by astrocytes of microglial cell-mediated neuroinflammation: effect on the activation of microglial signaling pathways. *Neuroimmunomodulation* 14, 168–174.
- von Bernhardi, R., 2007. Glial cell dysregulation: a new perspective on Alzheimer disease. *Neurotoxic. Res.* 12, 215–232.
- von Bernhardi, R., Eugenín-von Bernhardi, L., Eugenín, J., 2015. Microglial cell dysregulation in brain aging and neurodegeneration. *Front. Aging Neurosci.* 7, 124.
- von Bernhardi, R., Eugenín, J., 2004. Microglial reactivity to beta-amyloid is modulated by astrocytes and proinflammatory factors. *Brain Res.* 1025, 186–193.
- von Bernhardi, R., Tichauer, J., Eugenín-von Bernhardi, L., 2011. Proliferating culture of aged microglia for the study of neurodegenerative diseases. *J. Neurosci. Methods* 202, 65–69.
- von Bernhardi, R., Tichauer, J.E., Eugenín, J., 2010. Aging-dependent changes of microglial cells and their relevance for neurodegenerative disorders. *J. Neurochem.* 112, 1099–1114.
- Vorhees, C.V., Williams, M.T., 2006. Morris water maze: procedures for assessing spatial and related forms of learning and memory. *Nat. Protocols* 1, 848–858.
- Wyss-Coray, T., Mucke, L., 2002. Inflammation in neurodegenerative disease—a double-edged sword. *Neuron* 35, 419–432.
- Yamasaki, Y., Matsuura, N., Shozuhara, H., Onodera, H., Itoyama, Y., Kogure, K., 1995. Interleukin-1 as a pathogenic mediator of ischemic brain damage in rats. *Stroke; J. Cerebral Circulation* 26, 676.
- Yang, C.-N., Shiao, Y.-J., Shie, F.-S., Guo, B.-S., Chen, P.-H., Cho, C.-Y., Chen, Y.-J., Huang, F.-L., Tsay, H.-J., 2011. Mechanism mediating oligomeric Aβ clearance by naïve primary microglia. *Neurobiol. Dis.* 42, 221–230.
- Yang, R.B., Mark, M.R., Gray, A., Huang, A., Xie, M.H., Zhang, M., Goddard, A., Wood, W.I., Gurney, A.L., Godowski, P.J., 1998. Toll-like receptor-2 mediates lipopolysaccharide-induced cellular signalling. *Nature* 395, 284–288.
- Zhao, Q., Lu, J., Yao, Z., Wang, S., Zhu, L., Wang, J., Chen, B., 2016. Upregulation of Aβ42 in the Brain and Bodily Fluids of Rhesus Monkeys with Aging. *Journal of molecular neuroscience: MN.*